Top-Off Safety Analysis and Requirement of Hazard Mitigation for NSLS-II Facility

PS-R-ASD-RPT-DRV-001

Yongjun Li, Scott Buda, Raymond Fliller, George Ganetis, Richard Heese, Hsiao-Chaun Hseuh, Samuel Krinsky, PK Job, Brett Parker, Timur Shaftan, Sushil Sharma, Amy Xia, Lingyun Yang

12/15/2015

Contents

1. Executive Summary 1
1.1 Introduction to NSLS-II Accelerator Complex 1
1.2. Top-off Injection 2
1.3. Introduction to NSLS-II Beam-line Frontends 2
1.4. Radiation hazard associated with top-off injection 4
1.5. Credited apertures 5
- In beam-line front-ends: 5
- Credited apertures in the storage ring for ID beamlines 5
- Credited apertures in the storage ring for 3PW and bending magnet beamlines 5

1.6. Required interlocks 6
1.7. Response Time 6
1.8. Critical Devices 6
2. Top Off Injection Loss Dose Rate Analysis 8
3. NSLS-II Top-off Safety Simulation Study 11
3.1 Credited apertures for top-off safety 14
- In beam-line front-ends: 14
- Credited apertures in the storage ring for ID beamlines 14
- Credited apertures in the storage ring for 3PW and bending magnet beamlines 14

3.2 NSLS-II beam-lines 16
3.2.1 Insertion device beam-lines in 9.3m straight sections 17
3.2.2 Insertion device beam-lines in 6.6 m straight sections 18
3.2.3 Dipole beam-lines and 3PW beam-lines 19
3.2.4 Summary of credited apertures for NSLS-II beam-lines 20
3.3 Magnet parameter and needed scan ranges 21
3.3.1 Dipole magnet tuning range and shorts 21
3.3.2 Quadrupole, sextupole and corrector magnet tuning ranges and shorts 22
3.4 Magnet profiles 26
3.4.1 Dipole magnets 27
3.4.2 Quadrupole magnets 27
3.4.3 Sextupole magnets 28
3.4.4 Corrector magnets 28
3.4.5 Hard and soft edge magnet models 29

3.5 Injected beam initial conditions 29
3.6 Methodology 29
3.7 Simulation results 30
3.7.1 General considerations 30
3.7.2 Damping wiggler beam-line in long straight – XPD 31
3.7.3 Canted beam-line in short straight - SRX 34
3.8 Summary of simulations 40
4.TOSS Magnet Interlocks System Requirements 42
4.1 Magnet operating parameters requirements 42
4.2 Timing Requirements 44
4.3 Interlock Requirements 45
4.4 TOSS Interlock Design 47
4.5 Magnet Current Interlock 50
4.6 Storage Ring Dipole Voltage Interlocks 51
4.7 Isolation Amplifiers for Storage Ring Dipole Magnets 53
4.8 MicroController 56

1. Executive Summary

1.1 Introduction to NSLS-II Accelerator Complex

NSLS-II [1] is a state-of-the-art 3-GeV synchrotron light source at Brookhaven National Laboratory. The main parameters of the 3-GeV storage ring are summarized in Table 1.1

Table 1.1 Basic Parameters of the NSLS-II Storage Ring

Parameters [unit]	**Value**
Energy [GeV]	3
Circumference [m]	792
Number of DBA cells	30
Number of 9.3 m straights	15
Number of 6.6 m straights	15
Number of dipoles	60
Number of quadrupoles	300
Number of sextupoles	270
Circulating current at 3 GeV [mA]	500
Nominal bending field [T]	0.4

Due to a relatively short beam lifetime at full bunch intensity, (~3 hours), top-off operation is needed for the NSLS-II storage ring. Top-off operation maintains the stored beam intensity at a quasi-constant level, providing a constant thermal load on the beam-line optics, which is highly preferred by the user community. Injection disturbance will be very brief (tens of milliseconds) and occur about once per minute. A very robust and reliable injector composed of a 200-MeV LINAC, and a 3-GeV booster ring are able to deliver up to 15 nC per second of 3 GeV electrons. The main parameters of the booster ring are given in Table 1.2.

Table 1.2 Basic Parameters of the NSLS-II Booster Ring

Parameters [unit]	**Value**
Charge at Booster Injection [nC]	15
Injection energy [MeV]	200
Extraction energy [GeV]	3
Circumference [m]	158.4
Ramping repetition rate [Hz]	1
Total number of super-periods	4
Total number of bending magnets (combined function)	60
Total number of quadrupoles	24

1.2. Top-off Injection

The traditional way of operating a storage-ring based light source is in the "decay mode." In the decay mode, beam is injected into the storage ring with frontend safety shutters closed. Neither x-rays nor injected beam can enter the user beam-lines during injection. Once injection is completed, the stored beam current begins to decay due to beam loss from Touschek scattering, collision with residual gas, etc. The radiation flux and brightness are changing with stored beam current, as is the heat load on beam-line optics which impacts to quality of experimental data.

Top-off mode is to keep the stored beam current at a very stable level (within ±1%) by frequent injection with the front end shutters open. This mode of operation is supported by the design of the injection systems in most modern electron synchrotrons. Because stored beam intensity is maintained at a quasi-constant level and the shutters are continuously open, the x-ray flux to experiments and heat load on beam-line optics are kept highly stable, which is highly preferred by users.

The large design beam current of 500 mA which corresponds to a bunch charge of 1.25 nC and the low emittances of $\varepsilon_x < 1$ nm, $\varepsilon_y < 8$ pm, implies large Touschek scattering rates which limit the beam lifetime to approximately 3 hours. This short lifetime requires injection of 8 nC every minute to maintain the beam intensity with the specified limit of 1% of the peak intensity. The injection system is designed to provide a maximum capability of delivering up to 15 nC per booster cycle.

In order to make such a mode beneficial for synchrotron light users, the front end shutters which separate the accelerator from the photon beam lines must be kept open. Injection with open safety shutters introduces a special radiological risk caused by injected 3 GeV electrons which could enter the experimental floor via the open shutters during injection. This would cause unacceptably high radiation doses on the experimental floor, as illustrated in section 1.4. To guarantee the safety of top-off injection, we must assure that for all possible fault conditions, all errant injected particles are lost before a safe point within the storage ring tunnel. In NSLS-II, the upstream end-face of collimator #2 in the front ends is chosen as safe point. No injected beam can be allowed to pass through all physical collimators and enter the First Optics Enclosure (FOE). The purpose of this document is to describe and specify the additional safety measures that prevent charged particles from entering the photon extraction channel beyond this safe point.

1.3. Introduction to NSLS-II Beam-line Frontends

There are 30 straight sections in the NSLS-II storage ring. Fifteen have length 9.3 m and fifteen have length 6.6 m. One of the 9.3 m straights is used for injection and two others are occupied by or reserved for RF cavities. The 27 remaining straights will be used to accommodate various insertion devices (IDs). In the baseline of the NSLS-II construction project, there are six 3.4 m long damping wigglers (DWs) installed in three symmetrically located 9.3 m straight sections to reduce horizontal beam emittance from 2

nm to 1 nm. There are six baseline user ID beam-lines on six straight sections that are funded within the construction project. These beam-lines are listed in Table 1.3. Additional user beam-lines are presently under design. In the future, the fully built-out ring will have all 27 available straights occupied by insertion devices. A typical layout of then NSLS-II beam-line frontend is illustrated in Figure 1.1. In addition to insertion device beam-lines, there will also be dipole and three-pole wiggler (3PW) beam-lines.

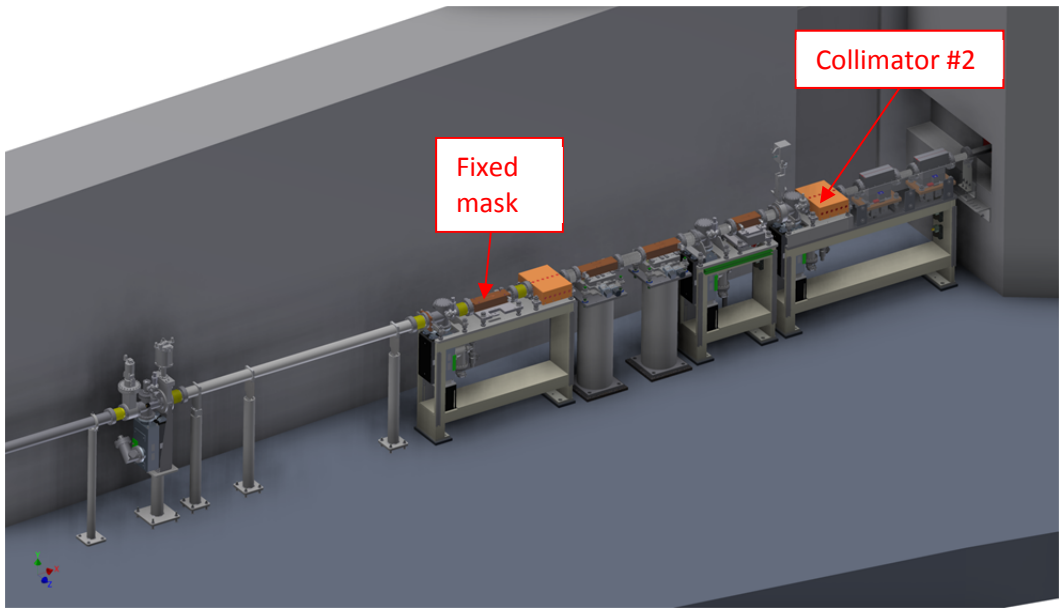

Figure 1.1 Typical NSLS-II beam-line front-end layout

In this report we have analyzed only the six NSLS-II project beamlines. We have also analyzed the preliminary design of a dipole/3PW beamline. All future beamline front ends and changes to existing front ends will be studied to assure they are safe for top-off injection.

Table 1.3 The NSLS-II baseline (Day One) beam-lines

Beam-line name	**Abbr.**	**Source**	**Canting angle (Unit: mrad)**
Inelastic X-ray Scattering	IXS	IVU [a]	None
Hard X-ray Nano-probe	HXN	IVU	None
Coherent Hard X-ray Scattering	CHX	IVU	None
X-ray Powder Diffraction	XPD	DW [b]	None
Coherent Soft X-ray Scattering, I and II	CSX	EPU [c]	0.16
Sub-micron Resolution X-ray Spectroscopy	SRX	IVU	2.00

[a] IVU – In Vacuum Undulator
[b] DW – Damping Wiggler
[c] EPU – Elliptically Polarized Undulator

1.4. Radiation hazard associated with top-off injection

The primary radiological safety issue for top-off injection with the safety shutters open is to assure that no injected electrons can pass through the apertures in the front-end and enter the First Optics Enclosure (FOE) on the experiment floor. The goal of the Top Off Safety System (TOSS) is to prevent this from occurring. Such an event is excluded for stored 3 GeV electrons, therefore our analysis and requirements focus on injected beam only. The radiation dose due to even one injected shot of 15 nC entering the FOE is considered unacceptable. The scenario that must be prevented is illustrated by the red trajectory in Figure 1.2.

In Figure 1.2, we plot the trajectories of the stored beam (blue), a lost injected electron following a safe trajectory (green), and a lost injected electron following an unsafe trajectory (red). The tracking studies described later in this report prove that the unsafe scenario cannot occur with the proper credited apertures and interlocks. In the figure, the vertical black lines represent physical apertures. The maroon parallelogram is a bending magnet; the purple rectangles are quadrupoles; the blue rectangles are sextupoles and the yellow rectangles are orbit correction magnets. A Cartesian coordinate system is used with the z-axis along the direction of the insertion straight and the x-axis in the perpendicular direction.

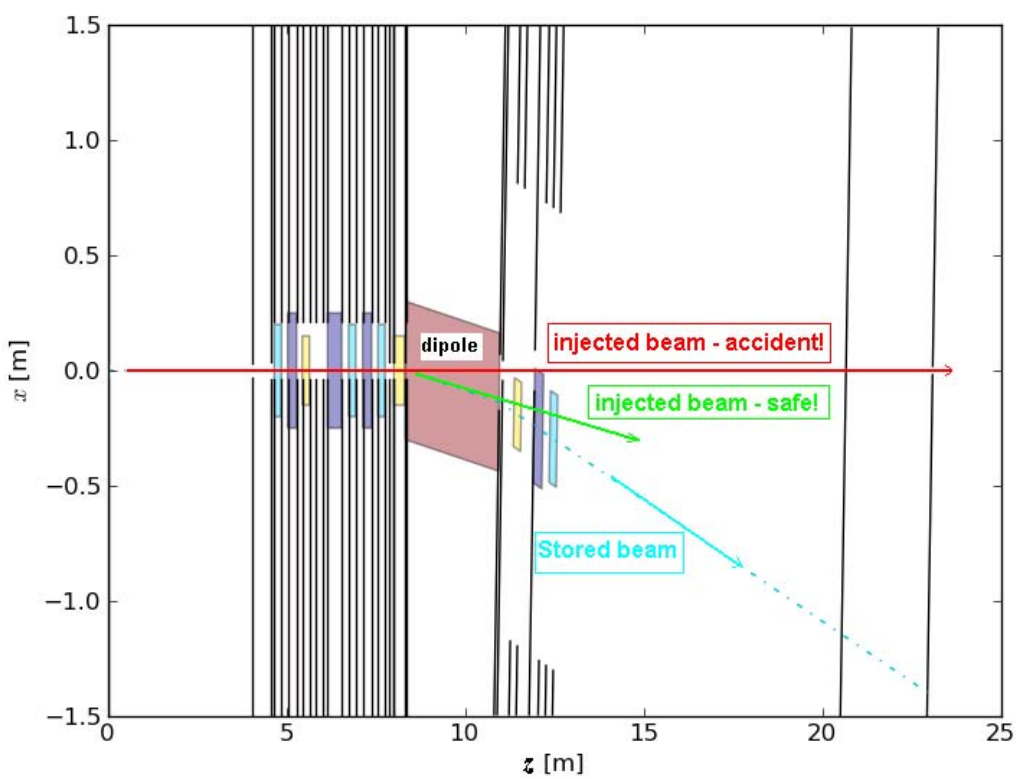

Figure 1.2 Safe and unsafe injected beam trajectories during top-off injection

If the full injected beam is conveyed to the FOE in the event of a complete failure of the top-off interlocks, the maximum total ambient dose-equivalent near the lead walls of the first optics enclosure, calculated by FLUKA, is approximately 80 mrem per pulse of 15 nC. This corresponds to 288 rem/h at full injection rate. The neutron dose equivalent rates are roughly 30% of the total dose at the lateral wall and >50% at the downstream wall of the FOE. Such high radiation dose means that the scenario of even one injected shot (15-nC charge) entering the FOE is not tolerable.

1.5. Credited apertures

After analyzing the possible machine failure scenarios and particle trajectory simulations, we identified the physical apertures that are critical to ensure safety during top-off operation once the required interlocks have been implemented. Justification of credited apertures and interlocks will be discussed later in this report. Our strategy to mitigate the potential hazards of top-off injection is to credit these apertures and introduce the necessary engineering and administrative configuration controls to ensure that these credited apertures are maintained in the proper position for top-off injection.

The credited apertures for NSLS-II top-off operation are listed below.

- In beam-line front-ends:
    - Collimator #2
    - Frontend fixed mask
- Credited apertures in the storage ring for ID beamlines
    - Synchrotron radiation absorbers (ABS-U or ABS-W)
    - The downstream flange on the S2 chamber for the electron beam
    - Blank-off flange terminating the antechamber for S2 chamber must be in place (no alignment tolerance)
- Credited apertures in the storage ring for 3PW and bending magnet beamlines
    - Crotch absorbers (ABS-C)
    - The downstream flange on the S4 chamber for the electron beam
    - Blank-off flange terminating the antechamber for S4 chamber must be in place (no alignment tolerance)
- Possible additional apertures as needed for specific beamlines

The detailed information of their locations and dimensions will be listed in Section 3.

All credited apertures will be fiducialized and aligned within a specified tolerance. To be conservative, misalignment errors due to installation, ground settling and thermal expansion have been taken into account in the simulations as the worst case (±2mm for the front-end components, and ±5mm for the storage ring apertures horizontally, and ±5mm longitudinally). That is, in simulations, aperture edges are always moved by 2 or 5 mm in the direction, which increases the aperture horizontally. The aperture

misalignment in the longitudinal direction is negligible for top-off safety, which has been coved by the horizontal misalignment.

1.6. Required interlocks

The following interlocks will be implemented to assure the safety of top-off injection:

- **Stored Beam Current Interlock**: This interlock prohibits top-off injection when the stored current is below 50 mA. The measurement accuracy for stored beam needs to be better than 10%. This interlock is employed since the presence of the stored beam with decent lifetime rules out many possible magnet errors. The stored beam current is monitored redundantly by two independent top-off current monitor systems, providing fast interlock outputs to top off system.

- **Storage Ring Dipole Current and Voltage Interlock**: This interlock prohibits top-off injection when the dipole magnet main power supply current and voltage fall outside a window of ±1% of its nominal value. Combining with the dipole trim power supplies capability, this interlock will assure each dipole field is within a specified window.

- **Injected Beam Energy Interlock**: This interlock prohibits top-off injection when the booster dipole power supply current falls outside a window of ±1% of the nominal extraction current. A simulation study [5] shows that if the dipole power supply currents in all three families are interlocked within a window of ±1%, the beam energy inside the booster ring is also confined in the same range.

- **Top-off Injection Current Interlock:** In addition, the top-off injection rate will be limited to 30 nC/min by an ACMI (Accumulated Charge Monitor Interlock) in each transport line. Each ACMI will trip the gun via the PPS system. In addition each ACMI will send a signal to the TOSS to inhibit Top Off. This will be in addition to the standard function of the ACMI to monitor other current limits.

1.7. Response Time

The time response requirement for the interlock to be activated is 15 ms, which means that top-off injection needs to be inhibited within 15ms after any requirements are violated. The determination of 15 ms response time is based on the considerations.

1. The storage ring dipole field decay rate when its power supply trips off;
2. The stored beam monitors' response time.

This requirement does not apply to the Top-off Injection Current Interlock.

1.8. Critical Devices

There are three devices which will be inhibited to stop injection during top off.

1. The booster extraction AC septum magnet
2. The storage ring injection AC septum magnet
3. The linac gun

The septa (items 1 and 2) will receive a trigger only if these interlocked conditions are fulfilled during top off. Without a trigger, these devices will not pulse. This will stop beam from being extracted from the booster, and subsequently injected into the storage ring.

The linac gun will be interlocked if the injected current exceeds top off injection current. No other top off conditions interlock the gun.

As an ALARA practice, and an operational aid, the TOSS will send a signal to the controls system to inhibit the electron gun pulse when it trips. This will stop the electrons from being injected into the booster and subsequently lost when the extraction septum does not fire. The gun pulse is already inhibited when the gun is interlocked, so no additional functionality is needed from the ACMIs to perform this.

Reference:

[1] NSLS-II PDR, http://www.bnl.gov/nsls2/project/PDR/default.asp

[2] L. Emery, M. Borland, Top-Up Operation Experience at the Advanced Photon Source, Proceedings of the 1999 Particle Accelerator Conference, New York, 1999, p 200.

[3] A. Ferrari, P.R. Sala, A. Fasso and J. Ranft, FLUKA- Manual, ITFN TC-05/11 (2005).

[4] S. Roesler and G. Stevenson, A FLUKA User Routine to Convert Fluence to Effective Dose and Ambient Dose Equivalent, CERN-SC-2006-070-RP (2006).

[5] T. Shaftan, Top-Off Mode Of Operations: Setting Limits On The Extracted Beam Energy By Constraining Currents Of Multiple Booster Dipole Power Supplies, IPAC2012, MOPPP060.

2. Top Off Injection Loss Dose Rate Analysis

Section 3 of this report will show particle tracking simulations for the NSLS-II ring that show an errant injected electron beam can be confined to the beam-line frontend inside the storage ring tunnel by use of appropriate apertures and interlocks. These tracking calculations show that no beam can be transmitted beyond collimator #2 or strike it within 5mm of the edge of the aperture. FLUKA Monte Carlo simulations have been performed to calculate the radiation levels in the occupied regions on the experimental floor due to the injected electron beam incident on collimator #2 or the upstream beam pipe. Ambient dose equivalent rates at the experimental floor for 15 nC/s injected beam incident on these components have been evaluated.

FLUKA simulations included 4 mis-steering injected beam scenarios:

Scenario1: Beam lost at 5 mm outboard side from the collimator #2 aperture.
Scenario2: Beam lost at 5 mm inboard side from the collimator #2 aperture.
Scenario3: Beam scraping outboard beam pipe 40 cm upstream of collimator #2.
Scenario4: Beam scraping inboard beam pipe 40 cm upstream of collimator #2.

The parameters in FLUKA model are summarized in Table 2-1.

Table 2.1 the parameters in FLUKA simulations

Collimator #2 aperture	X direction : +/- 3.96 cm	Y direction: +/- 1.42 cm
Ratchet wall collimator aperture	X direction : +/- 3.92 cm	Y direction: +/- 1.09 cm
FOE Lateral wall	139.7 cm from target with 18 mm Pb	
FOE Downstream wall	10 m from SR ratchet wall with 50 mm Pb	
FOE Scattering target	1” × 1” × 6” long copper rotated at 15 degree	
FOE bremsstrahlung stop	13.415 cm H × 9.06 cm V ×30 cm thick Pb	
FE and FOE Beam pipe	4” O.D. (outer diameter) with 2 mm Fe	

- *The apertures sizes in Table 3-1 are from 5ID SRX beamline, which has the largest aperture among 6 project beamlines.*

The dose rates from the above four mis-steering cases are summarized in Table 2.2 and in typical FLUKA dose plots of Figures 2.1 and 2.2.

Table 2.2 Dose rates from different mis-steering cases for 15 nC/s injected beam lost in front end. All doses are in mrem/hour.

		Scenario 1	Scenario 2	Scenario 3	Scenario 4
Injection rate 15 nC/s	FOE downstream wall	500	1000	700	2000
	FOE lateral wall	40	50	100	100
	SR @ corner	800	800	2500	1800
Injection rate 30 nC/min	FOE downstream wall	17	33	23	67
	FOE lateral wall	1	2	3	3
	SR @ corner	27	27	83	60

- *Note: in reality, the dose rate on FOE downstream wall will be much lower than Table 2-2 due to the collimators and secondary gas bremsstrahlung (SGB) shields in FOE, which are not included in FLUKA model for top off calculation.*

Figure 2.1 and 2.2 show typical dose rates for mis-steering scenario 4: beam scraping inboard beam pipe 40 cm upstream of collimator #2.

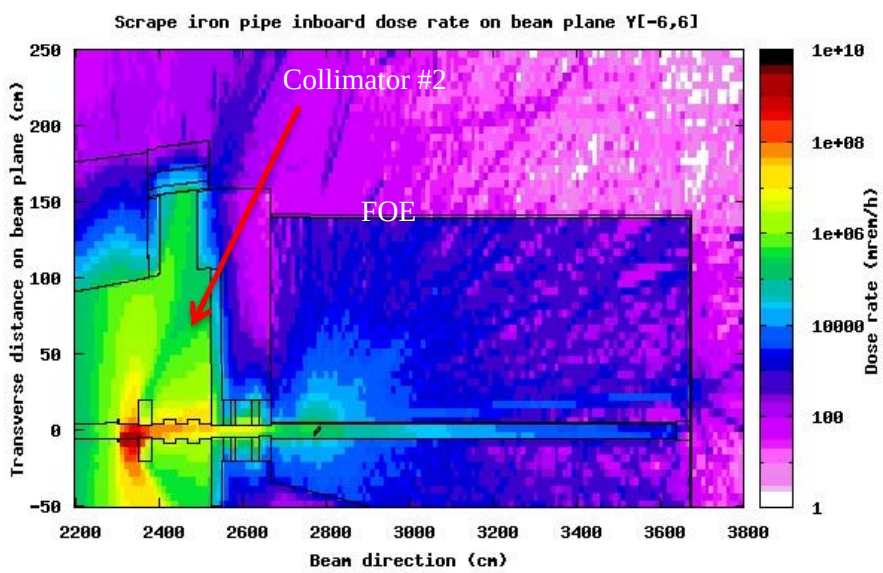

Figure 2.1 Dose rate on beam plane when electron beam scrapes steel pipe 40 cm upstream of collimator #2 at 15 nC/s

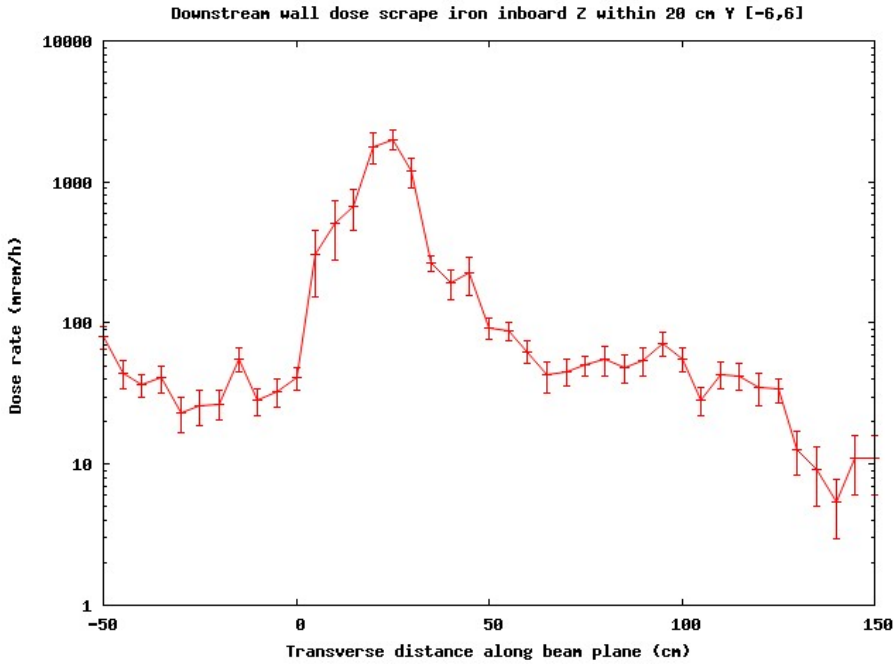

Figure 2.2 FOE downstream wall dose rate when electron beam scrapes steel pipe 40 cm upstream of collimator #2 at 15 nC/s. Note this calculation doesn't take credit of collimators and secondary gas bremsstrahlung (SGB) shields in FOE, which will reduce the dose rate significantly in reality.

The dose on the FOE downstream wall for scenario #4 is at the limit of the photon sciences shielding policy, and in all scenarios is unnecessarily high. The dose rate seen at the "storage ring corner" is near the maintenance door. This dose, though high in this scenario, is not particular to top off. This may occur during a fill with the photon shutters closed. Therefore it does not represent an additional hazard due to top off, whereas the doses external to the FOE is an additional hazard.

As these dose rates either exceed or come close to the photon sciences shielding policy in some cases and are unnecessarily high, we shall limit the injection rate to 30 nC/min during top-off. This will reduce all of the dose rates in the above table, a factor of 30. Therefore for all of the above mis-steering scenarios the dose will be less than 100 mrem/h. The necessary injection rate for top off is 8 nC/min, so reducing the injection rate from the full capacity of 15 nC/s to 30 nC/min during top off does not hamper the ability to successfully top off the machine, and provides sufficient overhead while keeping doses ALARA.

3. NSLS-II Top-off Safety Simulation Study

In order to establish the safety of top-off injection, we must show that with the implementation of specified interlocks and in-place credited apertures, no injected electrons can travel beyond the safe point and pass into the first optics enclosure (FOE). The safe point is the collimator #2's upstream aperture, which is located approximately 1.7 m away from the ratchet wall. The analysis to prove the safety of top-off injection requires multiple tracking simulations, scanning over all possible initial conditions (position, angle and energy) of injected beam and over all possible magnetic field configurations.

We use the backward tracking approach [1-3], in which the parameter scan is performed by tracking particles from the safe point in the beamline frontend back into the storage ring. The basic philosophy of backward tracking is that the trajectory of an electron going from one point to another in a pure magnetic field is the same as the trajectory of a positron moving in the opposite direction. Thus, if we can prove that no positron starting from the collimator #2 in the front-end can enter the acceptance of the ring chamber with all credited apertures and interlocks in place, we have proven that no electron starting from the ring acceptance can pass through the collimator #2 under the same conditions. Hence, we will have proven that no electron can travel past the collimator #2 and enter the first optics enclosure, which shows that top-off injection is safe.

In principle, particle tracking needs to be performed in both the horizontal and the vertical planes. However, for practical computational reasons, it is desirable to minimize the dimensionality of the initial conditions. An important assumption we use to simplify our analysis is to perform particle tracking only in the mid-plane. This approach has also been adopted by other light source facilities, like ALS and SRRL [2, 6]. As there are no strong coupling magnets in the storage ring, such as a large skew quadrupole or skew sextupole, the effect of being displaced vertically can be taken into account by increasing the scan ranges of magnets in tracking studies carried out in the mid-plane. This assumption greatly simplifies the geometry of the beam-line used in the tracking code and dramatically reduces computation time. In the following, when we discuss the geometry layout, unless otherwise stated, we always refer to the apertures in the horizontal mid-plane. Tracking in the mid-plane also requires that credited collimators must have maximum horizontal aperture in this plane, which is always true for the NSLS-II beam-lines.

In top-off safety simulations, we must consider electron trajectories that lie far from the ideal stored beam orbit (although their deviation is limited by the credited apertures). In this case, the magnetic field in the dipoles, quadrupoles and sextupoles can exhibit very nonlinear spatial dependence. In our simulation we were careful to properly take these nonlinearities into account in determining the electron trajectories in tracking studies.

The injected beam trajectory in the storage ring can be affected by many magnet parameters, which may vary. Some examples would be:

- Operator normal actions:
  - Choosing between several lattice configurations
  - Static one-time adjustment
  - Tuning during user operation
  - Optimizing injection timing to achieve more efficient injection
- Automated processes:
  - Orbit correction and feedback
  - Feed-forward compensation of optics perturbation from varying gap IDs
- Faults:
  - Magnet faults due to unexpected shorts inside coils or cooling water fault, etc.
  - Magnet power supply faults or trips
  - Incorrect setting by operators or corrupted machine setting files
  - Wrong polarity of magnet power supply

Possible magnet short scenarios include:

- Full or partial short of a single pole due to turn-to-turn or layer-to-layer insulation faults inside the coils
- External short across power terminators on a magnet that leaves coils for one or more poles without current

In addition, beam from the injector can be delivered to the storage ring with different initial conditions in energy, position and angle, which may be far away from their nominal values. For example, injected beam can have:

- Unmatched energy to the storage ring due to:
  - Booster ring dipole faults
  - Mis-trigging of booster ring's extraction system

- Abnormal incident angles or positions due to:
  - Booster-to-storage-ring transport line magnet faults
  - Mis-match of fast kickers and septa in strength and timing

To assure safety, the parameter scan for top-off safety tracking needs to be complete and conservative, covering all possible permutations of magnet settings and errors. For example, if there exist a total of k magnets in a beam-line from its start to end, and for each magnet we use n discrete set points to cover its continuous full-range excitations and faults, the number of magnet fault permutations is n^k. This exponential dependence makes it very time-consuming to perform a straightforward parameter scan. For this reason, we have introduced a new method of carrying out the parameter scan which is described in detail in the Physical Review ST-AB paper [7].

The approach we adopt is called the "cascaded parameter scan" method. Consider the beam-line mentioned above in regard to the conventional approach. After tracking initial particles to arrive at the first magnet entrance, we get a closed phase space area composed of an assembly of phase space points. The first magnet is assumed to have n set points covering all possible errors and excitations. We then track these particles through the

magnet for each of its *n* set points, and obtain *n* corresponding phase space areas at the magnet exit. We archive the coordinates *x* and *x'* of all of the particles in each subset for the purpose of retracing if necessary. Next we combine all the subsets into a superset using a repopulation technique in phase space. After obtaining the repopulated superset at the magnet exit, we use it as the input for subsequent tracking. The process of combining the subsets into a superset and repopulating it in phase space is repeated for the next magnets until the end of the beam-line is reached, or the defined apertures have stopped all particles.

In the cascaded parameter scan, if we simply combined all the particles in the subsets into a superset, the number of particles would increase exponentially with the number of magnet set-points, and the amount of computation would scale the same as for the conventional parameter scan. For a given area in phase space at the magnet entrance, the corresponding subsets for different excitations or errors at the magnet exit will usually have some overlaps, because we use discrete set-points to approximate a continuously variable magnetic field. It is easy to see that in the overlapped region, the density of particles becomes very high after many layers, and the distance in phase space between some particles becomes very small. These over-densely distributed particles represent conditions that are very close in phase space. Since we are studying a symplectic system, the area in phase space evolving under magnetic field is continuous and conserved. Therefore, an over-dense distribution of particles in phase space will not provide more useful information but just waste computation time by implementing redundant calculation. The purpose of adopting a repopulation technique is to avoid redundant tracking.

The implementation of repopulation is as follows: First, we combine all subsets at the magnet exit into a superset and define an area that can cover all the points in the superset. Then, we divide this area with a sufficiently small mesh grid. Next, all the particles in the superset are projected onto this mesh according to this rule: if there are any particles located with a grid (including on its borders), we will use the four points at the surrounding grid vertices to represent them. In the overlapping region of subsets, although the density inside a small rectangle can be very high, after repopulation four particles at the grid corners will adequately represent them. After the repopulation, the number of particles is proportional to the actual occupied area in phase space and not the number of magnet set points. In this way, we reduce the dependence of the number of tracking runs on the number of magnet set points from exponential to linear. More details of the repopulation technique are described in the published reference paper [7].

All the possible faults form a huge number of scenarios that need to be scanned. In the conventional top-off safety analyses, in order to decrease the number of permutations, magnet faults were categorized into different types according to their probabilities of occurrence and very unlikely events were excluded. For example, in the ALS and SRRL simulations, they assumed that only one magnet could be shorted at a given time because of its low probability. Using the cascaded parameter scan, we are able to include multiple low probability events simultaneously, which is more conservative.

The approach was benchmarked with other two top-off simulators developed for the ALS, and the SSRL facilities. Extremely good agreements have been achieved for the comparison on the trajectories on both single element passing and beam-line passing. In July 2011, a dedicated review was hold to review our approach. The committee composed of three external experienced reviewers from other laboratories reviewed this approach carefully. They concluded, "The newly-developed cascaded-scan approach is sound and provides a useful tool to quickly determine the requirements for top-up safety".

3.1 Credited apertures for top-off safety

In NSLS-II, specified apertures in the storage ring and beam-line frontends are credited for the purpose of top-off safety. Credited apertures must satisfy the following requirements:

- They must be fixed horizontal apertures;
- Maximum horizontal aperture must lie in the mid-plane;
- Radiation levels resulting from injected beam loss before the safe point during top-off injection must be acceptable;
- They must be fiducialized and aligned within a ±2mm (in the front-ends) or ±5mm (in the storage ring) tolerance[1];
- They must be under administrative control to assure they are maintained in the proper position.

As a result of extensive simulation studies, the following apertures are credited:

- In beam-line front-ends:
    - Collimator #2 (Figure 3.1)
    - Front end Fixed mask (Figure 3.1)
- Credited apertures in the storage ring for ID beamlines
    - Synchrotron radiation absorbers (ABS-U or ABS-W) (Figure 3.2b)
    - The downstream flange on the S2 chamber for the electron beam (Figure 3.2a)
    - Blank-off flange terminating the antechamber for S2 chamber must be in place (no alignment tolerance) (Figure 3.2a)
- Credited apertures in the storage ring for 3PW and bending magnet beamlines
    - Crotch absorbers (ABS-C)
    - The downstream flange on the S4 chamber for the electron beam(Figure 3.2a)
    - Blank-off flange terminating the antechamber for S4 chamber must be in place (no alignment tolerance) (Figure 3.2a)
- Possible additional apertures as needed for specific beamlines

Here Figure 3.1 is the same as Figure 1.1. This arrangement is just convenient to readers.

[1] Here the frontends and the storage ring having different error tolerance specifications are based on the achieved aperture tolerance in other facilities, e.g., the APS ring.

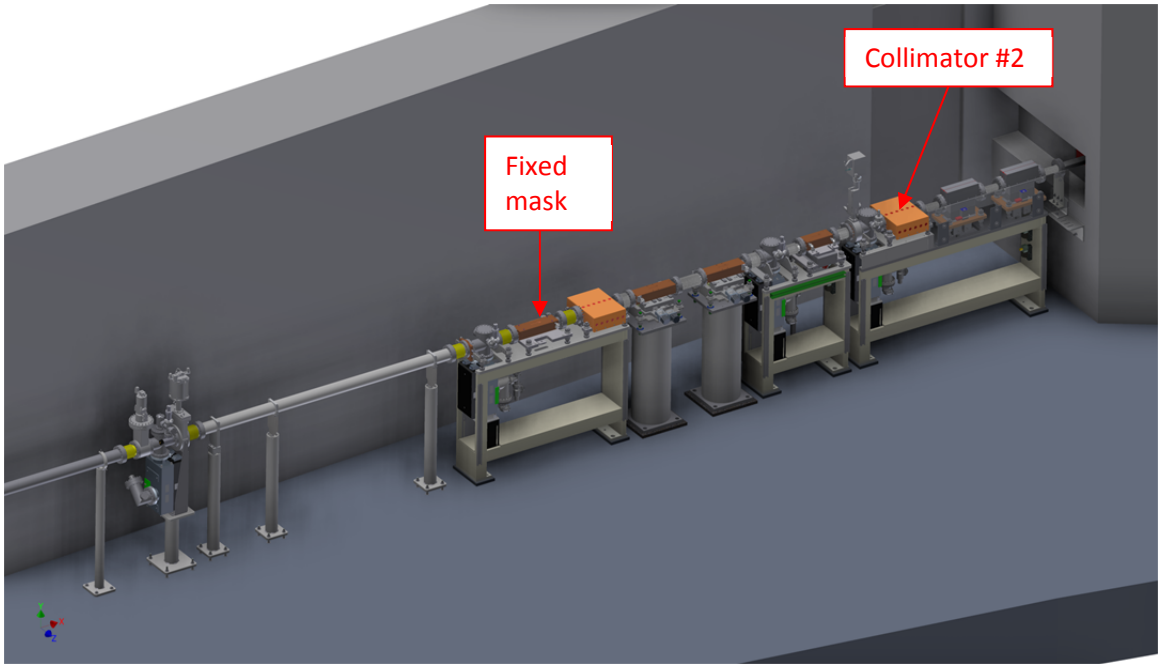

Figure 3.1 Typical NSLS-II beam-line front-end layouts

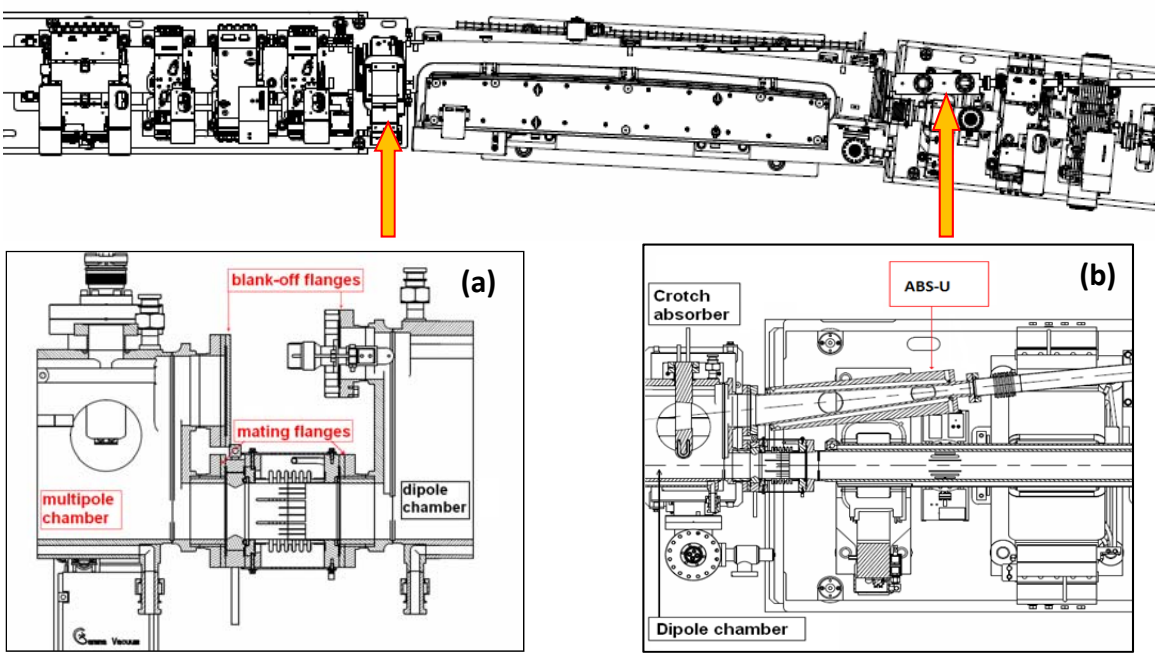

Figure 3.2 Credited apertures (marked in red text) in the storage ring. On the left (a), blank-off flange terminating the antechamber and mating flanges between multipole and dipole chambers. On the right (b), synchrotron radiation absorber ABS-U (for IVU and EPU) or ABS-W (for damping wiggler) downstream of the crotch. (the one shown in (b) is ABS-W)

The collimator #2 upstream end-face is the safe point, which means that injected beam

cannot be allowed to pass through it. It also defines the "starting point" for the backward tracking top-off safety analysis.

The credited apertures have distinct physical lengths in the longitudinal direction. When we mention transverse aperture dimensions, we refer to their downstream exits (relative to direction of stored beam) except the collimator #2, which its upstream aperture is credited.

3.2 NSLS-II beam-lines

According to the location of their source points, we categorize the NSLS-II beam-lines into three types:

- Insertion device sources in 9.3 m straight sections
- Insertion device sources in 6.6 m straight sections
- Dipole beam-lines or 3PW beam-lines

For each type, we carry out the analysis for one critical beam-line, i.e. one with the largest credited apertures. This is allowed because the apertures of other beam-lines fall within the largest apertures of the critical beam-line. Therefore, the safety analysis for the beam-line with the largest apertures is also valid for the others assuming the same magnet scan ranges.

If any new beam-line frontend is different from all existing beam-lines, we need to set up a new configuration to implement simulation.

Thus far, six project baseline beam-lines have been fully defined [4]. They encompass research programs in inelastic x-ray scattering (IXS), hard x-ray nano-probe (HXN), coherent hard x-ray scattering (CHX), coherent soft x-ray scattering and polarization (CSX), submicron resolution x-ray spectroscopy (SRX), and x-ray powder diffraction (XPD). All their source points are located in different straight sections. At present, our top-off safety analysis focuses on these baseline beam-lines. Additional beam-lines will be constructed in the future. We expect that most of the future NSLS-II beam-lines with source points from the IDs in straight sections will have very similar apertures to the baseline beam-lines. Therefore our approach to mitigate the hazards associated with top-off injection will work for them also. In case a particular beam-line will have such extremely large apertures that present interlocks are not sufficient, we have reserved drift space with sufficient length in the frontends to accommodate a sweeper magnet to deflect any incident electron beam. If such a sweeper magnet is required, it will need to be designed.

There will also be beam-lines with source points in the dipoles or Three Pole Wigglers (3PWs). At present, these beam-lines are in an early stage of design. Based on the preliminary designs, we believe that our approach to top-off safety will be applicable to them. More detailed studies will be performed in the future. Preliminary analysis shows that the safety for this type of beam-line is assured under the same interlocks as we have considered for the ID beam-lines at straight sections.

3.2.1 Insertion device beam-lines in 9.3m straight sections

Two project baseline beam-lines have their source points located in 9.3 m long straight sections. They are XPD (cell 28 straight) and IXS (cell 11 straight setion). The XPD's source point is comprised of damping wigglers (totally 2 × 3.4 m in length), and the IXS's source point is from an In Vacuum Undulator (IVU). So far no canted IDs are located in 9.3m straight sections in the baseline project.

Damping wiggler (XPD)

The layout of a damping wiggler beam-line is shown in Figure 3.3. All apertures are marked in black as slots. These include: the storage ring vacuum chamber in the straight section and the mating flange between dipole and multipole chambers; the blank-off flanges terminating the antechambers; the downstream exit of the SR absorber which is located downstream of crotch absorber; the fixed mask and the collimator #2 which are located in the beam-line frontend.

The magnets that can affect electron trajectories for the beam-lines between the collimator #2 and ID are:

- 4 sextupoles (blue): SM1, SH4, SH3 and SH1
- 4 quadrupoles (purple): QM1, QH3, QH2, QH1
- 3 horizontal orbit corrector magnets (yellow): CM1, CH2 and CH1
- 1 dipole magnet (brown): B1

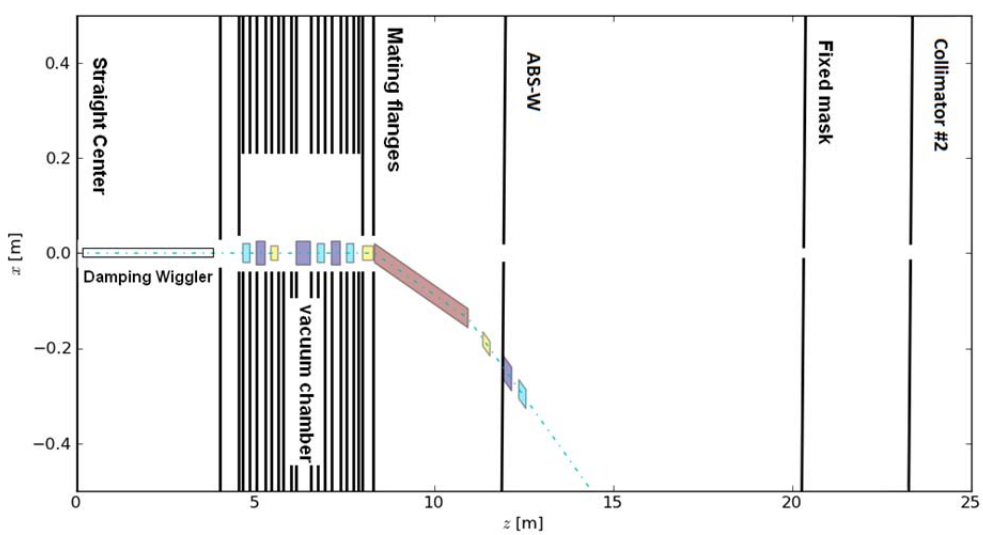

Figure 3.3 Damping wiggler beam-line layout. The colored blocks represent the magnets: SH1, QH1, CH1, QH2, SH3, QH3, SH4, CH2, B1, CM1, QM1, and SM1 (from left to right)

Undulator beam-lines (IXS)

The apertures for this beam-line fall within those of the XPD beam-line. Therefore, the safety analysis for XPD is valid also for IXS (see Section 3.7.2.1).

3.2.2 Insertion device beam-lines in 6.6 m straight sections

Four baseline beam-lines use IDs in the 6.6 m straight sections. They are HXN, CHX, CSX and SRX. Of these, HXN and CHX are non-canted beam-lines, while CSX and SRX are canted.

Canted undulator beam-lines (CSX and SRX)

The layout of the CSX beam-line (with a canting angle 0.16 mrad) is shown in Figure 3.4. The SRX beam-line has a similar layout as the CSX, but with a large canting angle 2.0 mrad. The SRX's fixed mask has two separated openings. To be conservative, in simulation we use a full aperture covering both openings to define the initial conditions for backward tracking.

The magnets that affect electron trajectories for the beam-lines between the collimator #2 and ID are:

- 4 sextupoles (blue): SM1, SL3, SL2 and SL1
- 4 quadrupoles (purple): QM1, QL3, QL2, QL1
- 3 horizontal orbit corrector magnets (yellow): CM1, CL2 and CL1
- 1 dipole magnet (brown): B1

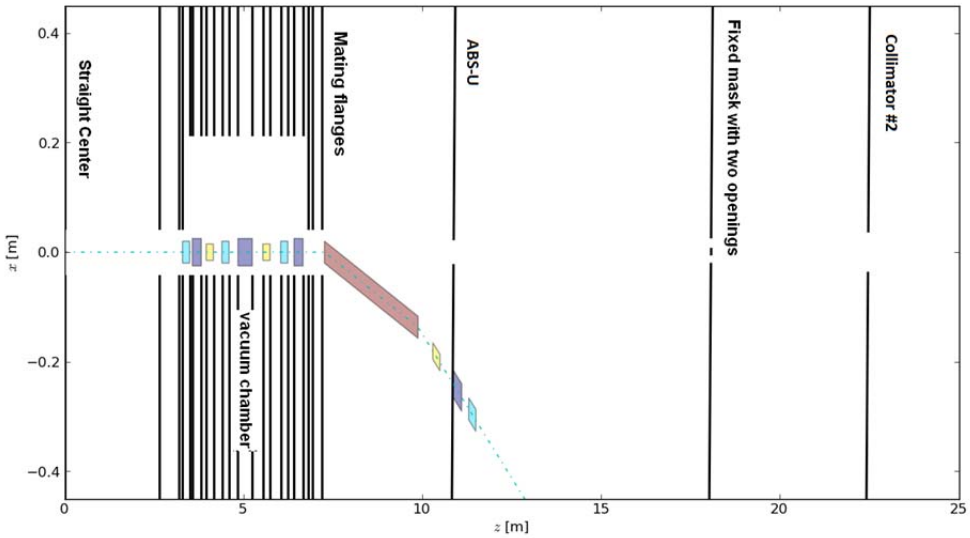

Figure 3.4 SRX beam-line layout. The colored blocks represent the magnets: SL1, QL1, CL1, SL2, QL2, CL2, SL3, QL3, B1, CM1, QM1, and SM1 (from left to right). The canting magnets located in the straight are not shown here, because no particle can travel this far into straights in the backward tracking.

Non-canted undulator beam-lines (HXN and CHX)

Two non-canted beam-lines, HXN and CHX are included in the project baseline. The apertures for these beam-lines lie within those for the canted devices so the top-off safety analysis for the canted beam-lines applies to the non-canted ones (see Section 3.7.3.1).

3.2.3 Dipole beam-lines and 3PW beam-lines

A dipole beam-line's nominal source point is located 2.125 mrad from the upstream end of the second dipole magnet of the DBA cells. Three Pole Wigglers (3PWs) will be installed upstream of the second dipoles in the DBA cells. Both dipole and 3PW beam-lines are using the same type extraction port (crotch absorber). The crotch absorber and frontend are at an early stage of design. Based on the preliminary designs, we find that they are safe under the same interlocks as the ID beam-lines.

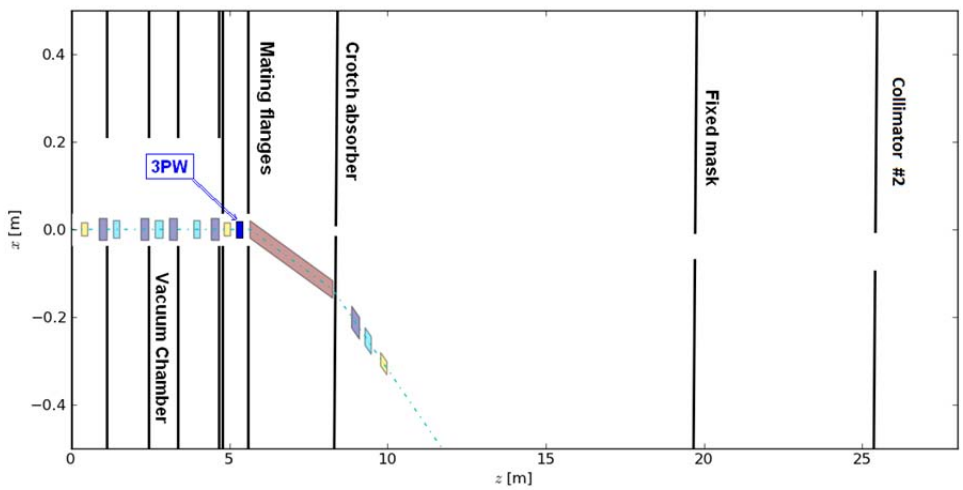

Figure 3.5 Dipole/3PW beam-lines layout. The colored blocks represent the magnets: CM1, QM1A, SM1A, QM2A, SM2, QM2B, SM1B, QM1B, CM2, 3PW, B2, QH3, SL3, QL3 and CL2 (from left to right, the last three elements can also be CH2, SH4 and QH3). The position of fixed masks and collimator #2 will depend on radiation source.

The magnets that affect electron trajectories for the beam-lines between the collimator #2 and ID are:

- 4 sextupoles (blue): SM1A, SM1B, SM2 and SL3 (or SH4)
- 5 quadrupoles (purple): QM1A, QM2A, QM2B, QM1B, QL3 (or QH3)
- 3 horizontal orbit corrector magnets (yellow): CM1, CM2 and CL2 (or CH2)
- 1 dipole magnet (brown): B1 – the second dipole in the DBA cells
- 1 three-pole-wiggler (dark blue – only for 3PW beam-lines): 3PW

3.2.4 Summary of credited apertures for NSLS-II beam-lines

The details of credited absorbers for the NSLS-II beam-lines are summarized in Table 3.1.

Table 3.1 Horizontal apertures associated with top-off safety

beam-line name		XPD	IXS	HXN CHX [f]	CSX	SRX	BM/3PW
cell No.		28	10	3/11	23	5	TBD
canting angle (mrad)		none	none	none	0.16	2.0	none
specified vacuum chamber on multipole girds	location [a]	straight section	straight section	straight section	straight section	straight section	straight section
	dimension (mm)	-38/+210	-38/+210	-38/+210	-38/+210	-38/+210	-38/+210
mating and blank-off flanges	location	between multipole and dipole chambers	between multipole and dipole chambers	between multipole and dipole chambers	between multipole and dipole chambers	between multipole and dipole chambers	between multipole and dipole chambers
	dimension (mm)	±38	±38	±38	±38	±38	±38
ABS-C[b]	location (m)	N.A.[h]	N.A.	N.A.	N.A.	N.A.	3.1
	dimension (mm)	N.A.	N.A.	N.A.	N.A.	N.A.	+8/-16
ABS-U [c]	location (m)	11.88	11.44	10.20	10.20	10.20	N.A.
	dimension (mm)	±15	±15	±15	±15	±15	N.A.
fixed mask [d]	location (m)	20.32	20.32	19.07	19.07	17.89	13.98
	dimension (mm)	±11.38	±5.28	±4.97	±5.35	±5.00/ ±4.34 [g]	±14.80
collimator #2 [e]	location (m)	23.53	23.53	22.24	22.24	22.24	19.68
	dimension (mm)	±36.57	±36.57	±36.57	±36.57	±36.57	±21.88

[a] Aperture locations are relative to the upstream straight section centers for ID beam-lines, and the second DBA dipole's upstream end face for dipole/3PW beam-lines
[b] ABS-C Crotch Absorber – thus far, only credited for dipole/3PW beam-lines
[c] ABS-U - Synchrotron Radiation Absorbers – downstream aperture
[d] Fixed Mask (FM) – downstream aperture
[e] Collimator #2 – upstream aperture
[f] CHX and HXN have the same configuration, so they are listed together.
[g] SRX has two openings on its fixed mask to accommodate two canted IDs
[h] Not Applicable for Top Off Safety

3.3 Magnet parameter and needed scan ranges

For typical layout of the NSLS-II ID beam-lines, there are about 12 to 13 magnets affecting trajectories in backward tracking. The determination of magnet scan ranges is based on consideration of the characteristics of magnet power supplies. Possible human error, such as incorrect magnet polarity settings, has also been included. The basic philosophy is to assure that the choices of scan ranges are sufficiently conservative to cover the worst scenarios.

3.3.1 Dipole magnet tuning range and shorts

The NSLS-II storage ring contains 60 dipole magnets. Of these, 54 have 35-mm gap (small gap) and 6 have 90-mm gap (large gap). The main circuit for the dipole coils is in series and each dipole has its own trim circuit. The dipoles' main power supply current will be interlocked within ±1% of its nominal value. Each 35-mm gap dipole has a trim coil whose power supply will be restricted to provide another ±1.5% of the main PS nominal current. Therefore, the total allowed tuning range from its power supply is ±2.5%. The 90-mm gap dipoles have trim coils with power supplies restricted to provide ±3% of its nominal value. Therefore, in this case the total allowed tuning range from its power supply is ±4%.

Let us now consider the effect of inner coil shorts on the dipole field. Our dipole magnets are C-shaped planar dipoles, i.e. no transverse gradient. Inner coil shorts will change field intensity, but the change on the field profile will be negligible. In our simulations, for dipoles, we always use the same profile whenever we consider power supply faults or coil shorts. Once there are any layer-to-layer or turn-to-turn shorts, the power supply current keeps unchanged, but the voltage on the shorted dipole coil terminators is reduced. The dipole voltage interlock system measures the voltage across each dipole magnet. The voltage signal for each dipole in every cell will be used to calculate a difference signal and a total signal for each magnet. These three signals will be digitized in a safety rated micro-controller. The micro-controller will determine if the voltage is within the required limits. The system shall be designed to resolve a difference in a single magnet of 1%. In simulation, to be conservative, the case of single turn short was taken into account. A single turn short in the 35mm dipole can cause about -3% field's drop-off. Therefore the total scan range to cover a single turn short, plus the allowed tuning range of the power supply for 35mm dipole is from -5.5% up to 2.5%. The 90 mm dipoles will have separate voltage detection on each pair; therefore they will have the same percentages and a windows width for voltage comparison. A single turn short can lead to about 1% field's drop-off (each 90mm dipole is 84 turns). Then the total scan range for this type magnet can be taken from -5% to 4%.

In summary, the scan range for 35mm dipoles is taken to be from -5.5% up to +2.5% of its nominal value, which includes the possibilities of single turn-to-turn short, power supply interlock and trim coil's contribution. The step-size for scanning is 0.5%. For the 90mm dipoles, in addition to the ±1% power supply interlock, we need to include the ±3% contribution from their trim coils and -1% from a single turn short. The total scan

range is taken to be from -5% to +4%, with a step-size of 0.5%. The reason to choose 0.5% step-size is that coil's turn-to-turn shorts can result in partial shorting of a single turn.

3.3.2 Quadrupole, sextupole and corrector magnet tuning ranges and shorts

Scan ranges from power supply

Except for the dipole power supply current and voltage, the storage ring magnet power supplies will not be interlocked for top-off safety. Un-interlocked magnet power supply faults (trips) at accelerator facilities are frequent enough to be treated as part of "normal" operation. The magnet strength will sweep the entire range of values between the initial set-point and zero. Also, operators can set magnet strengths above their initial set-point by mistake. Therefore, the possible tuning ranges of magnets are determined by their power supply capacities. Table 3.3 shows the nominal tuning range for the different types of magnets and the worst case range for highly unlikely power supply fault. To be conservative, the widest scan ranges (the worst case) for all these magnets (last column in Table 3.3) have been chosen to define the magnet scan ranges in our simulations. In Table 3.3, Quad/Sext 1-3 represent quadrupoles/sextupoles in the zero-dispersion sections and Quad/Sext M1-2 represent quadrupoles/sextupoles inside the dispersion sections.

Table 3.3 NSLS-II Magnet allowed tuning ranges by power supplies

Magnet Type	PS current Max. (A) [a]	PS I Max Fault (%) over Magnet I Max.
Quad 1&3	176.0	30
Quad 2	177.0	37
Quad M1	185.0	42
Quad M2	238.0	45
Sext 1,2,3& M1	125.0	30
Sext M2	167.0	25
Alignment Correctors	25.0	43

[a] Power Supply I Max. is the absolute maximum current the power supply could achieve if there were multiple faults of the power supply regulator. All power supply and controls interlocks would have to fail for this condition to happen.

Scan range increase due to incorrect polarity

Although each individual magnet polarity will be measured, in our simulations we make a conservative assumption that all the quadrupoles and sextupoles can be set with wrong polarities. This enhances the robustness of our analysis. Extending magnet scan ranges to include wrong polarity is also based on the fact that such an event has been observed at other light source facilities[2]. Hence, we take the quadrupole and sextupole tuning ranges

[2] M. Borland (ANL): Incorrect sextupole polarity was found in APS ring once.

to extend from the negative maximum to positive maximum strength independent of their nominal polarities.

Orbit corrector magnets themselves have bi-polar power supplies and can deflect the beam in both in- and out-board directions, which has been taken into account in the simulation.

Scan range increase due to off-axis plane motion

As already noted earlier, we carry out tracking only in the mid-plane. The effect of beam's vertical offset is included by an increase of magnet scan ranges. The maximum field intensity occurs in the vicinity of magnet poles. The vertical offset is limited by the gap height (±5mm) in the region between antechamber and beam chamber (Figure 3.6). We have calculated the field profile on the ±5mm off-axis planes using the electromagnetic field code Opera2-3D. The example in Figure 3.7 shows the normalized field profile representing the NSLS-II 66-mm quadrupole and sextupole. The nominal profile in the mid-plane is shown as well. We found the peak field intensity in the off-axis plane is about 7% larger than in the on-axis plane. Therefore we extended the magnet scanning range by an additional 10% in order to properly account for this vertical offset field variation without the need of tracking the particle also in the vertical plane. A similar scenario applies to the case of sextupoles.

As for orbit corrector magnets, their deflecting angle is only ±0.8 mrad. We didn't calculate their detailed field profiles on the off-axis planes, but increased their scan range from 143% to 150% to cover this effect.

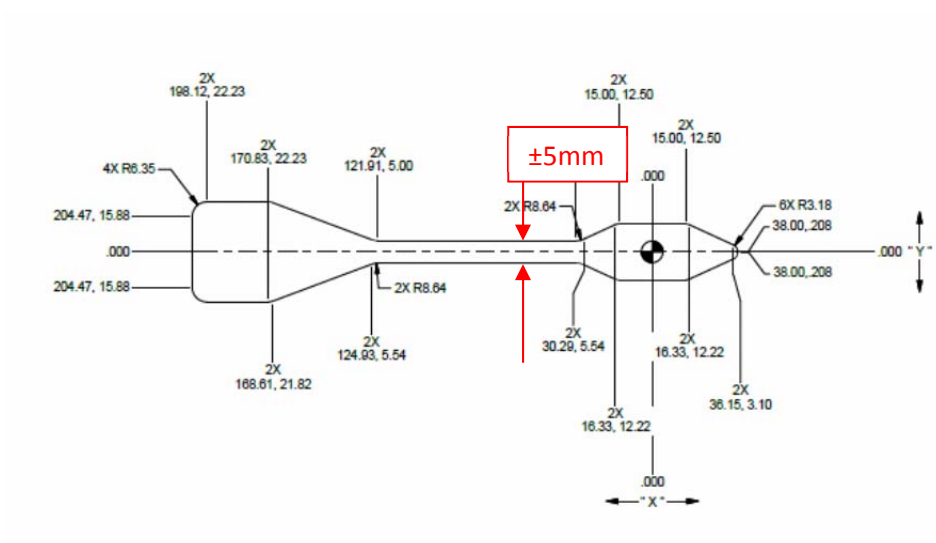

Figure 3.6 Vacuum chamber cross-section profiles for multipole section. The maximum beam's vertical offset is limited by the height of the gap connecting beam chamber and antechamber.

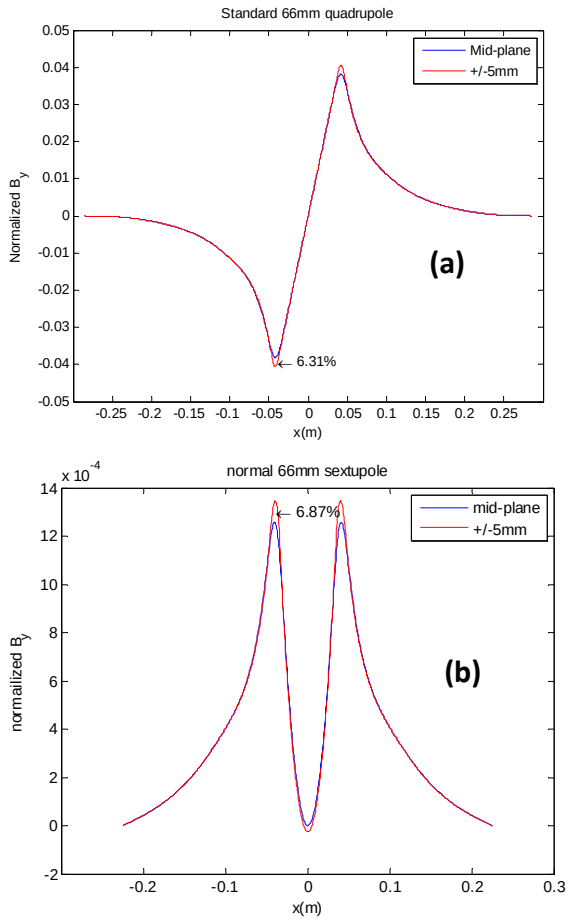

Figure 3.7 Quadrupole (a) and sextupole (b) field profiles at off-axis plane

Magnet saturation

In defining the scan ranges of magnet excitations, we ignored magnet saturation effects at large excitation current. In other words, the magnet field magnitudes are assumed to increase linearly with their excitation currents, while their normalized field profiles are assumed to be unchanged[3]. This assumption is conservative because in this way we always scan wider ranges than actual cases where saturation occurs in the magnets.

Multipole magnet shorts

In addition to their power supply faults, multipole magnets can be shorted during normal operation. We only consider the shorts that occur in a single pole coil. The shorts between different poles are excluded. The reason for such choice is due to the fact that we adopted a design to prevent shorts between different coil terminators during manufacturing process. All the NSLS-II quadrupole and sextupole magnet terminators for different poles are protected by an isolated transparent Lexan cover (Figure 3.8). Therefore, simultaneous shorts by external conductors on different poles are extremely

[3] A. Jain (BNL): The change of magnetic field profile with the excitation current is very small in NSLS-II multipoles.

unlikely events. For single-pole shorts, we only consider the cases for a magnet to have a single partial (50%) and full (100%) shorted pole[4]. The shorts can occur at different poles; due to the transverse symmetry we consider that a quadrupole could have 4 types of shorts, and sextupole could have 6 types (see the last column of Table 3.4). The profiles for the multipole magnets missing one pole have been calculated by OPERA2d and shown in Figure 3.10b and 3.11b.

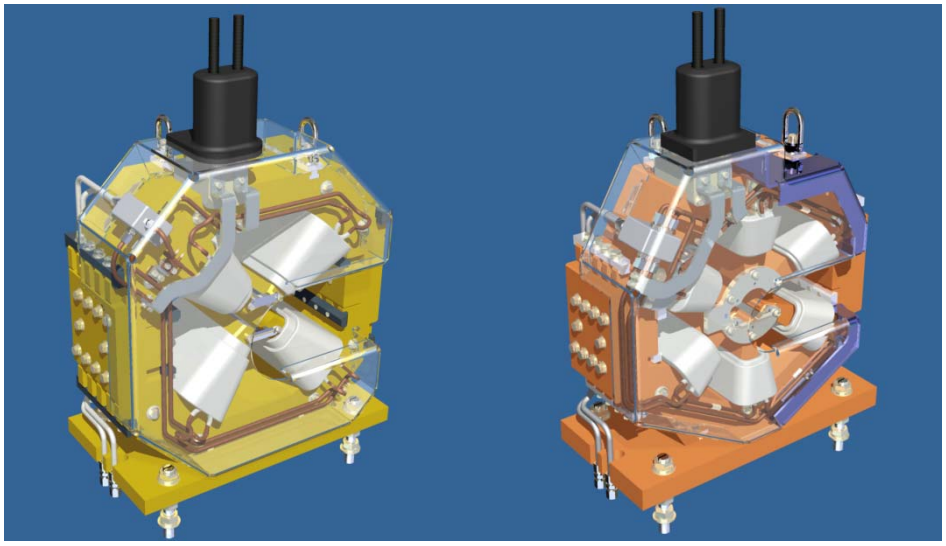

Figure 3.8 Prevention of magnet terminator shorts

In the cascaded parameter scan, we include the possibility that any magnet can be shorted simultaneously. That is, in addition to scanning over the range of magnet strengths, we also include the possibility of shorts. Although a scenario with multiple shorted magnets at the same time is a very unlikely event, our method can still take them into account [7]. We also scanned the multipole shorts at different excitation currents, which make our analysis be independent of the storage ring optics.

In Summary, the total scan ranges of quadrupole, sextupole and corrector magnets, which include their power supply faults, wrong polarity settings, and beam vertical displacement, are shown in Table 3.4.

[4] A coil short in-between could be simulated using interpolation of the fields between field maps that were computed for fully-shorted turns.

Table 3.4 Magnet scan ranges and shorts

Parameter	Lower boundary	Upper boundary	number of short types [a]
Energy of Injected Beam	-4%	4%	
B1(35mm)[mrad]	104.72×94.5%	104.72×102.5%	included
B1(90mm)[mrad]	104.72×94.5%	104.72×104.5%	included
QH1 K_1 [m^{-2}]	-2.2×140%	2.2×140%	4
QH2 K_1 [m^{-2}]	-2.2×150%	2.2×150%	4
QH3 K_1 [m^{-2}]	-2.2×140%	2.2×140%	4
QM1 K_1 [m^{-2}]	-2.2×150%	2.2×150%	4
QM2 K_1 [m^{-2}]	-2.2×150%	2.2×150%	4
QL3 K_1 [m^{-2}]	-2.2×140%	2.2×140%	4
QL2 K_1 [m^{-2}]	-2.2×140%	2.2×140%	4
QL1 K_1 [m^{-2}]	-2.2×140%	2.2×140%	4
SH1 K_1 [m^{-2}]	-40×140%	40×140%	6
SH3 K_2 [m^{-3}]	-40×140%	40×140%	6
SH4 K_2 [m^{-3}]	-40×140%	40×140%	6
SM1L K_2 [m^{-3}]	-40×140%	40×140%	6
SM2 K_2 [m^{-3}]	-40×140%	40×140%	6
SM1R K_2 [m^{-3}]	-40×140%	40×140%	6
SL3 K_2 [m^{-3}]	-40×140%	40×140%	6
SL2 K_2 [m^{-3}]	-40×140%	40×140%	6
SL1 K_2 [m^{-3}]	-40×140%	40×140%	6
CH1 [mrad]	-0.8×150%	0.8×150%	Included
CH2 [mrad]	-0.8×150%	0.8×150%	Included
CL2 [mrad]	-0.8×150%	0.8×150%	Included
CL1 [mrad]	-0.8×150%	0.8×150%	Included
CM1 [mrad]	-0.8×150%	0.8×150%	Included

[a] The shorted coil can be located in different poles. Therefore the shorted profiles are different, which are defined as short types. For quadrupoles, the possible short types are: (1) 50% shorted pole in quadrant 1 or 4, (2) 100% shorted pole in quadrant 1 or 4, (3) 50% shorted pole in quadrant 2 or 3, (4) 100% shorted pole in quadrant 2 or 3. For sextupoles, two more types are needed: (1) 50% shorted pole in upper or lower plane, (2) 100% shorted pole in upper or lower plane. The profiles are same for the two cases in which the shorted poles are symmetric with the mid-plane.

3.4 Magnet profiles

Magnet field profiles in the mid-plane and ±5mm off the mid-plane have been calculated by the electromagnetic field solver - OPERA 2D [5]. The field maps cover the region in the horizontal plane, which is defined by credited aperture dimensions. Inside this region, the magnet field is quite nonlinear. A numerical integrator (Adams integrators) with a fine longitudinal step-size is used to obtain accurate trajectories.

3.4.1 Dipole magnets

The dipole magnet is the most critical element in top-off safety analysis. We use its 2D-profile in the mid-plane (the x–z plane) to include its fringe field to carry out accurate particle tracking. Figure 3.9 shows the normalized dipole field profile in the mid-plane. Because NSLS-II dipoles do not have a design gradient, the field variations due to vertical offsets are negligible. We don't need to increase its scan range to including particle's offset in the vertical plane like other multipoles.

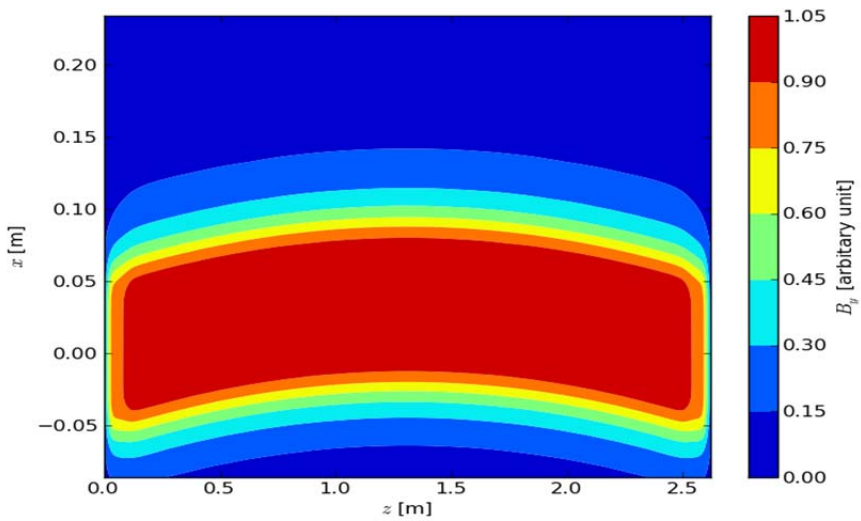

Figure 3.9 Normalized NSLS-II 35mm dipole 2d field profile in the mid-plane

3.4.2 Quadrupole magnets

There are three types of field profiles to represent quadrupoles with different apertures: 66mm without ears, 66mm with ears, and 90mm. Their normalized field profiles are shown in Figure 3.10a. Figure 3.10b shows the field of a quadrupole with one right coil fully and partially shorted[5]. To simulate the effect of magnet shorts we substitute a shorted field map for the normal one in the affected magnet, which is also applied in simulating sextupole shorts.

[5] According to symmetry, the profile of a shorted coil in the left plane is represented by the mirror image of a short in the right plane, which is also applied for sextupole shorts.

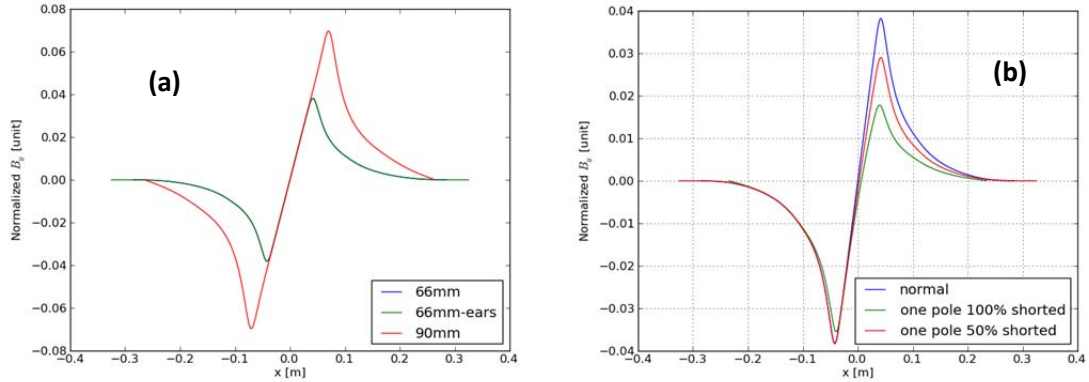

Figure 3.10 Quadrupole field profiles. (a) Normal status: the profiles of 66mm w/o ears are overlapped (blue and green). 90mm is in red. (b) Single shorted pole: 0%, 50% and 100% shorted pole in quadrant 1 or 4.

3.4.3 Sextupole magnets

There are also three normalized field profiles to represent sextupoles with different apertures (Figure 3.11a). Figure 3.11b gives their profiles with one pole shorted.

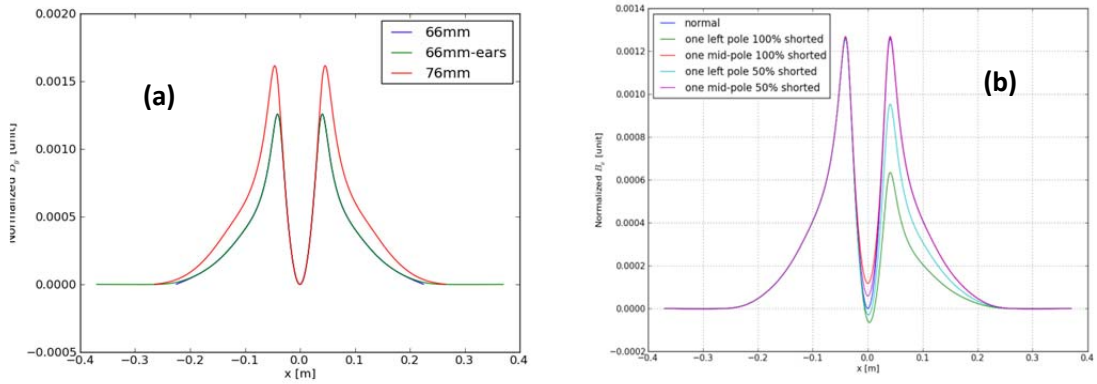

Figure 3.11 Sextupole field profiles. (a) Normal status: the profiles of 66mm w/o ears are overlapped (blue and green). 76mm is in red. (b) Single shorted pole: 0%, 50% and 100% shorted pole in quadrant 1 or 4.

3.4.4 Corrector magnets

The closed orbit corrector magnet normalized profile is shown in Figure 3.12. We assume that the change of its profile due to shorted coils is negligible. When we scan over the range defined by their power supplies, all shorts have been included automatically.

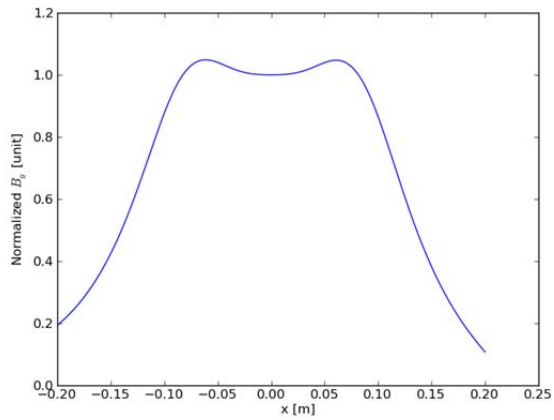

Figure 3.12 Corrector magnet field profil**e**

3.4.5 Hard and soft edge magnet models

The dipole magnet is represented by a soft edge model (i.e. 2D profile) and the quadrupoles, sextupoles and correctors are approximated by hard edge models (i.e. 1D profile) in the longitudinal direction. The purpose of using different models for different magnets is to save the computation time without loss of accuracy in calculating particle trajectories. A comparison between 1D (hard edge) and 2D (soft edge) carried out in ALS shows that it is appropriate to use 1D model for quadrupoles for this purpose [2].

3.5 Injected beam initial conditions

Particle trajectories depend upon the initial conditions (position, angle and energy). The two credited apertures, fixed mask and collimator #2 located at the magnetic field free region in the frontends, define a parallelogram determining the initial *x-x'* phase space for backward tracking [2]. Booster ring's dipole power supplies (two families defocusing dipoles and one family focusing dipole) will be interlocked to confine the injected beam energy deviation within ±1%. In simulation we scanned over the energy range of ±4% with a step-size 1%.

3.6 Methodology

As mentioned earlier, we employ the cascaded parameter scan (CPS) technique to carry out backward tracking [7]. With backward tracking, one starts at the safe point (in NSLS-II, it is the collimator #2 upstream end) and tracks virtual particles towards the storage ring. The basic philosophy of backward tracking is: if no positron can be tracked from beam-line into storage ring acceptance, then no electron can travel in the opposite direction. In this manner, we demonstrate that no injected beam from the storage ring can exit the beam-line and enter the first optics enclosure. The backward tracking method was introduced in the analysis of the APS top-off safety at Argonne National Laboratory, and has been widely adopted by many other facilities, including ALS at Lawrence Berkeley National Laboratory.

The top-off safety analysis for each beam-line follows these steps:

1. Specify the starting point (collimator #2 upstream end-face) and the endpoint (center of ID straight section).
2. Identify credited apertures that limit the positions and angles of electron trajectories.
3. Impose the misalignment errors on the credited apertures.
4. Identify all magnetic field and electron beam parameters that affect trajectories.
5. Implement parameter scan to detect if there exist any unsafe scenarios.
6. Restrict parameters by interlock systems or tighten credited apertures to eliminate unsafe scenarios if they exist.
7. Characterize the robustness of the solution with respect to parameter changes beyond the interlock limits.

3.7 Simulation results

3.7.1 General considerations

For each beam-line, backward tracking using the cascaded parameter scan technique was used to analyze safety. The credited apertures with specified tolerance were incorporated into the tracking runs, and scans were carried out over injected beam energy and magnet parameters. As we shall discuss, with the installation of the credited apertures and the implementation of the interlocks on storage ring and booster dipole currents (or voltage) as well as on the storage ring electron beam current, the analysis proves that top-off injection is safe for the NSLS-II storage ring.

For backward tracking, the initial beam positions and angles are limited by a parallelogram in phase space defined by the dimensions of collimator #2 and fixed mask apertures. Numerous particles[6] are populated within the parallelogram for the tracking study. Beam energy has been scanned with a fixed step-size of 1% within the range of ±4%. All credited apertures are located in the proper longitudinal location and their horizontal aperture is increased by 4 mm (in the frontends) or 10 mm (in the storage ring) full, i.e. outside edge moved out by 2 or 5 mm and inward edge move in by -2 or -5 mm.

The magnet-strength scan ranges that we used for the simulations are shown in Table 3.4. No quadrupole or sextupole magnets are interlocked. It is good that we do not need to interlock these multipole magnets because:

- The flexibility of wide magnet tuning range is kept, which is beneficial for possible machine upgrade in the future.
- It reduces the cost of interlock system. All NSLS-II quadrupoles are powered independently. Interlocking on each individual quadrupole would be costly.

The criteria for judging a beam-line's safety is that no initial particle can be tracked back into the storage ring acceptance beyond a specified location – the endpoint. For ID beam-lines with source points at the straight sections, we choose the midpoints of straight

[6] The number of particles is usually chosen to be several millions. It depends on the convergence of phase space areas. More details can be found in [7].

sections as their endpoints. For dipole/3PW beam-lines, we choose the upstream dipole's exit ports as their endpoints. It is not necessary to track virtual particles back to the injection point, as any errant particle must be in the storage ring acceptance prior to the beamline in question.

Among the beam-lines in the long straights (9.3m), the damping wiggler beam-line (XPD) is the most challenging, because it has the largest apertures (~ ±1.0mrad). Demonstrating the safety of the XPD beam-line during top-off injection, also assures the safety of other long straight section ID beam-lines with more restrictive apertures under the same interlocks on the injected beam energy and the dipole field. This principle is also applied for the beam-lines in the short straights (6.6m), in which the canted SRX beam-line turns out to be the most critical one.

3.7.2 Damping wiggler beam-line in long straight – XPD

3.7.2.1 Cascaded parameter scans results

The initial particle positions and angles at the starting point (collimator #2) for backward tracking are defined by the dimensions and the distance in-between of collimator #2 and fixed mask, see Figure 3.13.

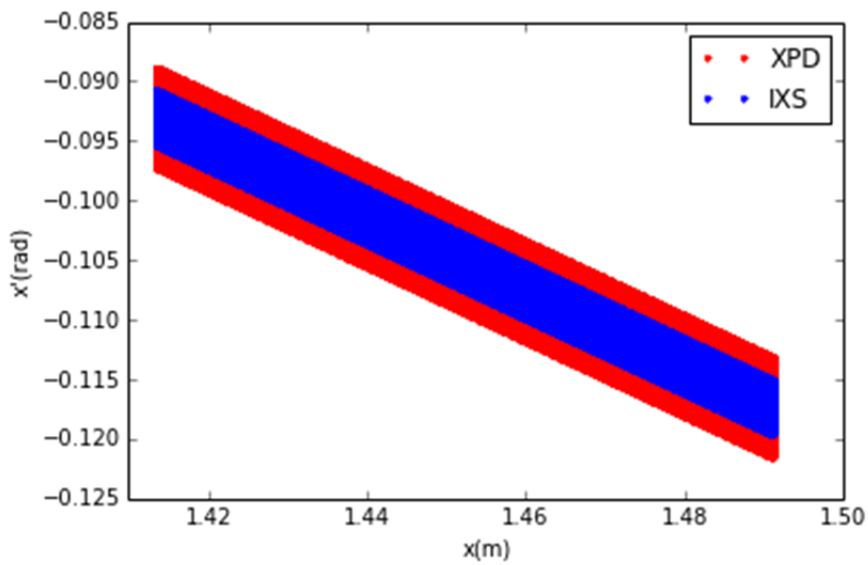

Figure 3.13 Particles initial conditions at the same longitudinal position (collimator #2) for the XPD (in red) and IXS (in blue) beam-lines, where ±2mm misalignment errors have been included to widen the apertures. Here the coordinates are relative to the stored beam orbit. The analysis to assure the safety of the XPD is also valid for the IXS.

The magnet strengths are scanned over the full ranges specified in Table 3.4. The electron beam energy deviation is also scanned over ±4% with the fixed step-size of 1%. Figure 3.14 shows the backward trajectories envelope obtained from cascaded parameter scan. Even under the worst possible mis-steered particle conditions and magnet faults, the backward trajectories cannot pass through the sextupole SH4, the nearest multipole to the

dipole B1. This demonstrates the safety of top-off injection for the XPD beam-line and hence also for IXS.

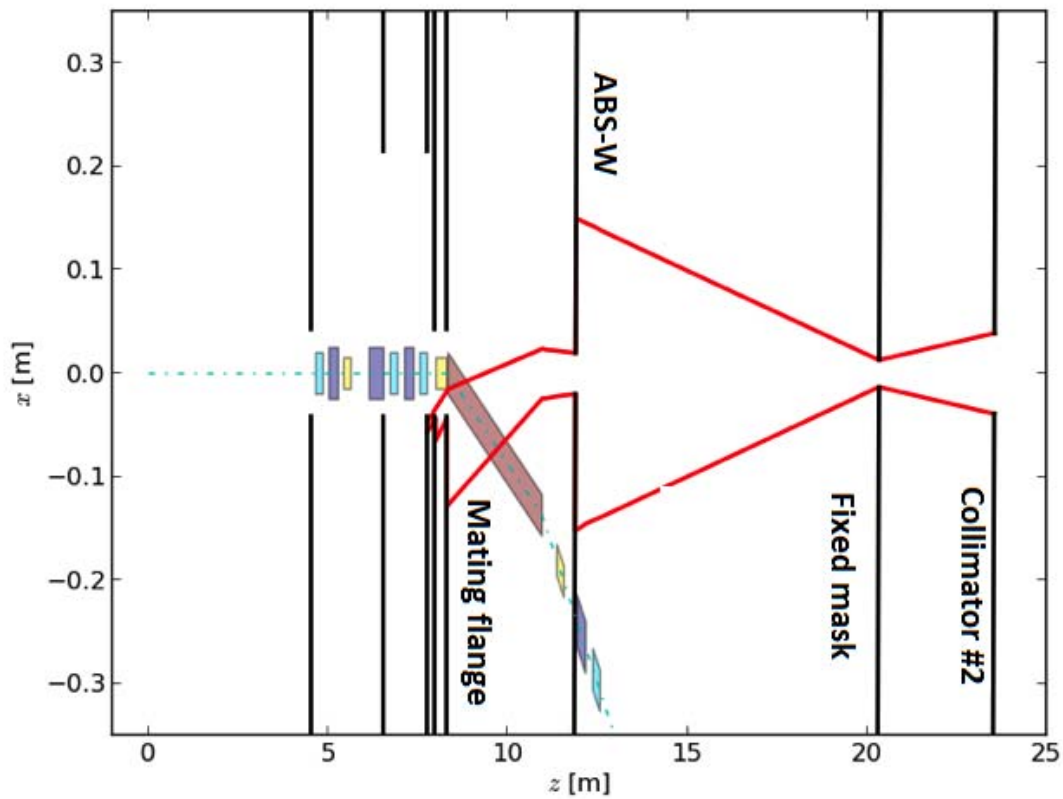

Figure 3.14 Envelop of backward tracking trajectories for the XPD beam-line. It shows that all particles starting from the collimator #2 are not able to enter the storage ring acceptance with the existence of credited apertures in place. The apertures from right to left are collimator #2, fixed mask, damping wiggler synchrotron radiation absorber, and mating flange, multipole vacuum chamber.

3.7.2.2 Robustness (safe margin) of interlocks

Dipole power supply current interlock

The robustness (safe margin) of the interlock on dipole power supply current has been checked by extending the dipole field scan range beyond the interlock limit. If the dipole is overpowered, injected beam will get stronger deflection to the ring side, which increases top-off injection safety. Only if the dipole field is reduced beyond a certain value, top-off injection could become unsafe.

From simulation, we have found that only if the dipole field is reduced below 80% of its normal value, could injected beam possibly be extracted from the storage ring (Figure 3.15) and pass into the first optics enclosure. Since our interlocks on dipole power supply

current and voltage restrict the dipole field within a much narrow window (±2.5% for 35mm dipoles and ±4.0% for 90mm dipoles) around its normal value, the safety margin of dipole field is quite large In mean time, the interlocks on the dipole current and voltage are also needed in order to assure the energy of electrons extracted from the booster and those stored in the storage ring are properly matched. Next we will discuss the robustness of beam energy interlock.

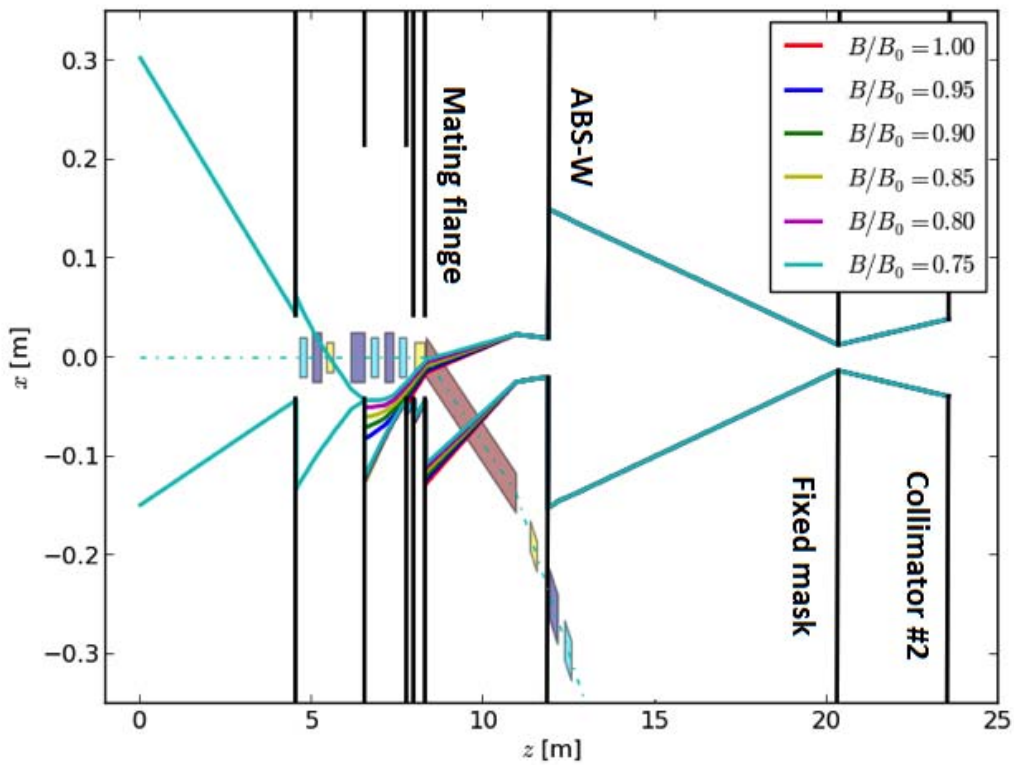

Figure 3.15 Robustness of dipole field interlock for the XPD beam-line. Only when the dipole field drops off below 80% of its nominal value, can injected beam be extracted from the ring acceptance.

Injected beam energy interlock

The robustness of the injected beam energy interlock has been studied in a similar way. In the case when the dipole scan range is limited within its interlock window, we tracked particles with an energy deviation up to 10% higher than the nominal value, and found that the beam-line is still safe (Figure 3.16). Lower beam energies will be deflected to the inside of the storage ring and are therefore not a concern. Since the energy interlock will confine the energy deviation to be below ±4%, the safety margin is also very large.

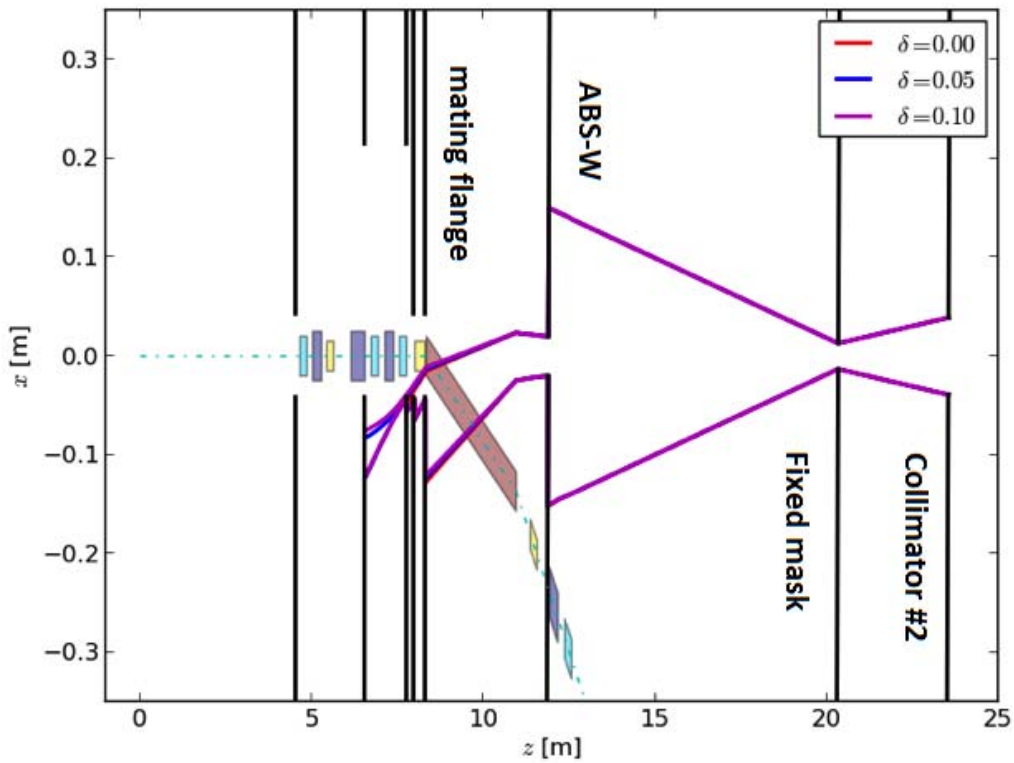

Figure 3.16 Robustness of injected beam energy interlock for the XPD beam-line. Even when beam energy is 10% above 3GeV, the beam-line configuration is still safe.

3.7.3 Canted beam-line in short straight - SRX

3.7.3.1 Cascaded parameter scan results

For this beam-line, there are two openings in the fixed mask to accommodate two IDs with a canting angle of 2 mrad. Therefore the initial particle conditions in phase space are two separated parallelograms as shown in blue in Figure 3.17. In our calculation, we used a larger parallelogram shown in red to cover the two separated parts. The extended area in phase space also includes the initial conditions of the non-canted beam-lines (HXN and CHX) and small canting angle beam-line (CSX) located in other three short straights. Demonstrating the safety of the SRX beam-line with extended initial condition area also assures the safety of other short straight section ID beam-lines with more restrictive apertures under the same interlocks on the injected beam energy and the dipole field.

The trajectory envelope for the SRX beam-line from the backward cascaded parameter scan is shown in Figure 3.18. The extreme ray in the worst case will be stopped by the vacuum chamber after passing the sextupole SL3.

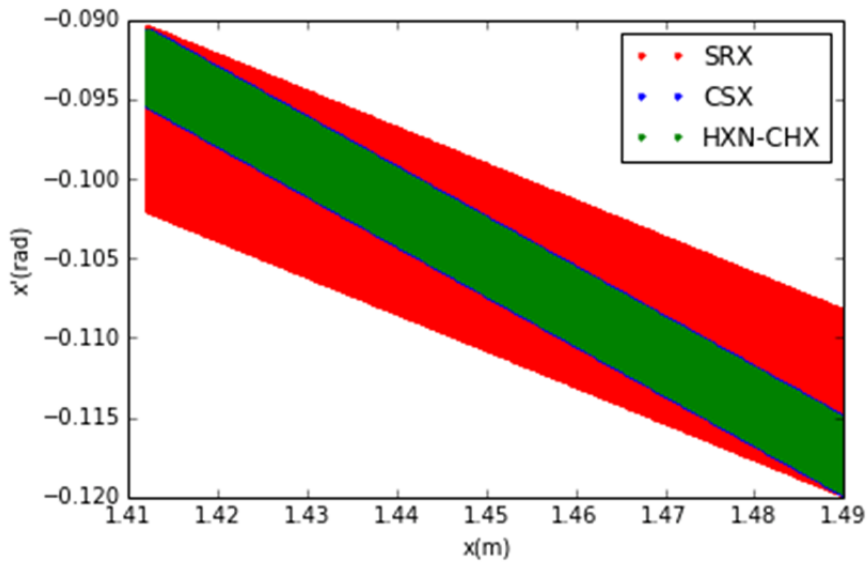

Figure 3.17 Particle initial conditions in phase space for short-straight beam-lines. The biggest parallelogram in red corresponds to an extended opening covering two holes in the fixed mask of SRX. The parallelogram in blue represents the initial condition for the CSX with 0.16 mrad canting angle. The green is for two non-canted beam-lines – HXN and CHX. The big parallelogram in red is used to cover both canted and non-canted beam-lines.

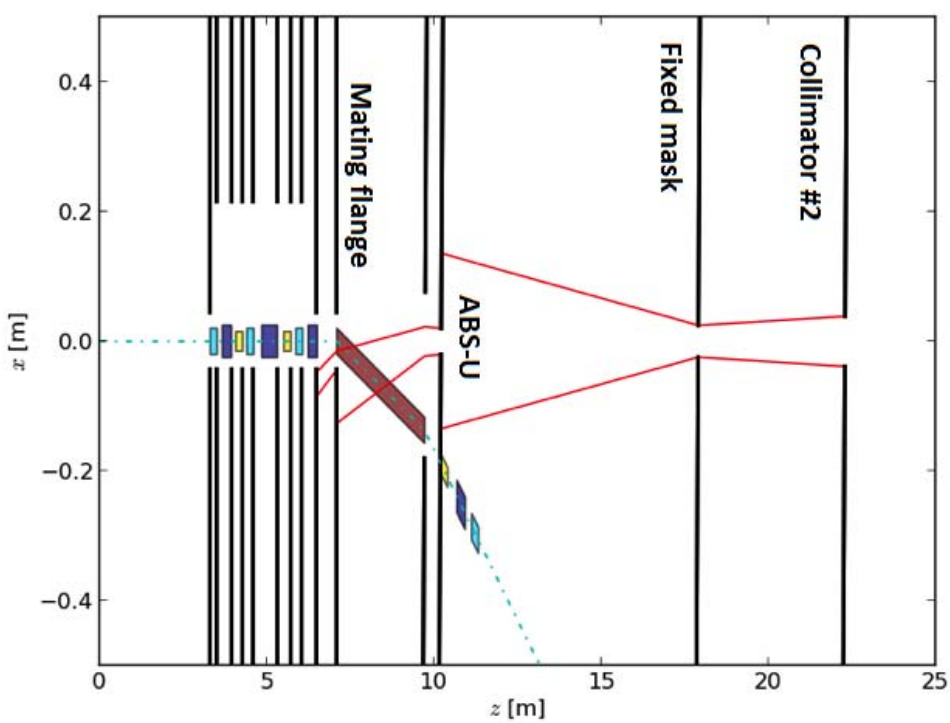

Figure 3.18 Envelop of backward tracking trajectories for the SRX beam-line

3.7.3.2 Robustness of interlocks

In this case, the robustness of dipole and injected beam energy interlocks are again checked by extending their scan ranges beyond the interlock limits as shown in Figure 3.19 and 3.20. If the injected beam energy is interlocked, it was found that it is still safe even when dipole field drops off 25% below the set-points. Next we assumed the dipole field was interlocked, and extended the injected beam energy deviation up to 10% of the nominal value, it turns out to be still safe. Lower beam energies will be deflected to the inside of the storage ring and are therefore not a concern.

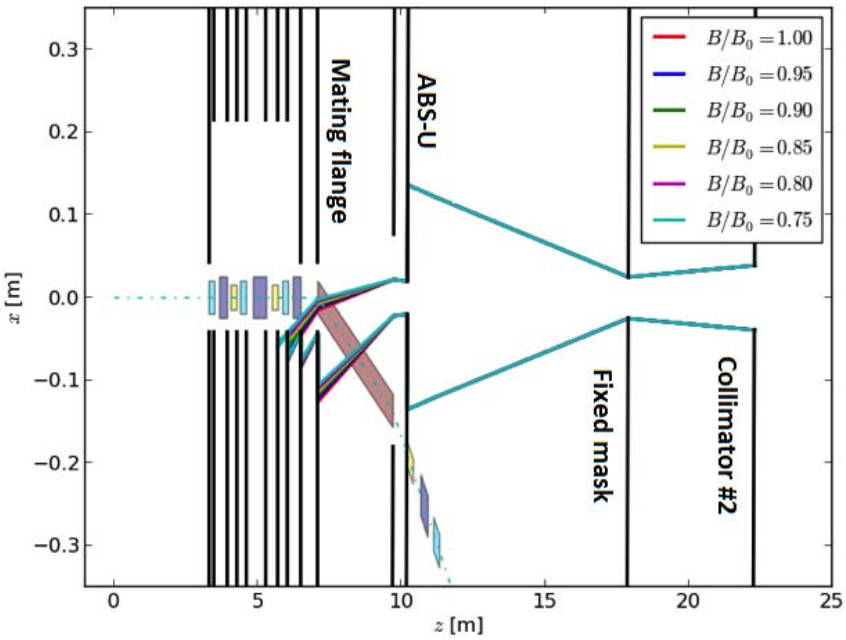

Figure 3.19 Robustness of dipole field interlock for the SRX beam-line. No beam can be extracted from the ring acceptance even when dipole field drops off 25% below the set-points.

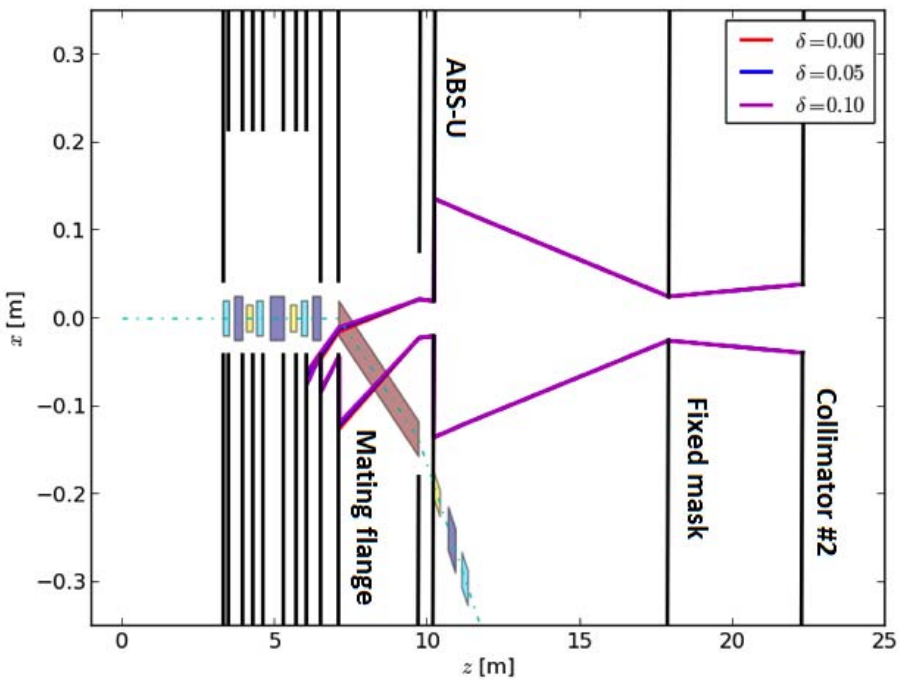

Figure 3.20 Robustness of injected beam energy interlock for the SRX beam-line

3.7.4 Dipole/3PW beam-line

3.7.4.1 Cascaded parameter scan results

Although no dipole/3PW beam-line is funded in the project baseline, they will be constructed in the future. We need to ensure their safety under the same interlocks as the baseline beam-lines. The following top-off analysis is based on the preliminary design efforts on dipole/3PW beam-lines. We are using one of the dipole beam-lines as an example to prove that it is safe. Once the dipole/3PW beam-line designs reach an advanced stage, the top-off safety analysis for them will be completed.

The initial particle positions and angles at the starting point are defined by the collimator #2 and fixed mask, as shown in Figure 3.21. Up to ±4% energy deviations have been scanned with the fixed 1% step-size. The dipole beam-line with current aperture configurations and specified interlocks is safe during top-off operation. Figure 3.22 shows the backward trajectories envelope obtained from cascaded parameter scan. Even under the worst possible mis-steering particle conditions and magnet faults, the backward trajectories cannot pass through the quadrupole SM1B, the nearest quadrupole to dipole B1. This type beam-lines are actually safer than the ID beam-lines. This is because the crotch aperture outboard aperture, which defines the worst-case trajectory, will be only 8mm (see Section 3.8).

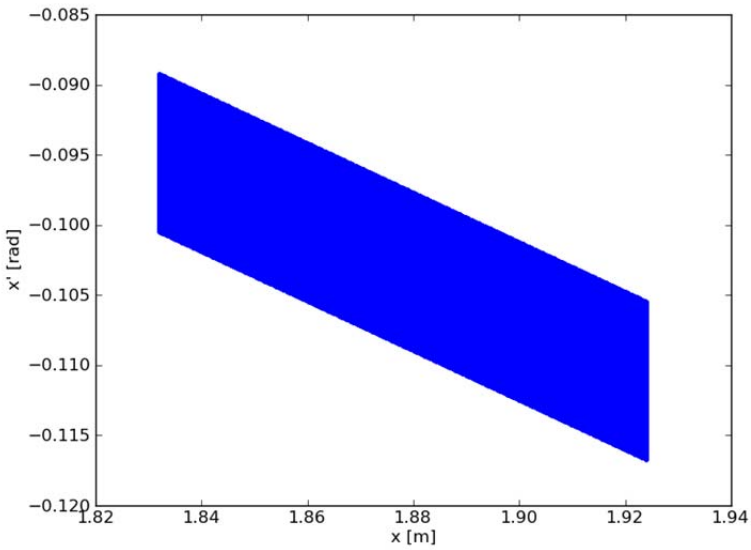

Figure 3.21 Particles initial conditions in phase space for dipole beam-line

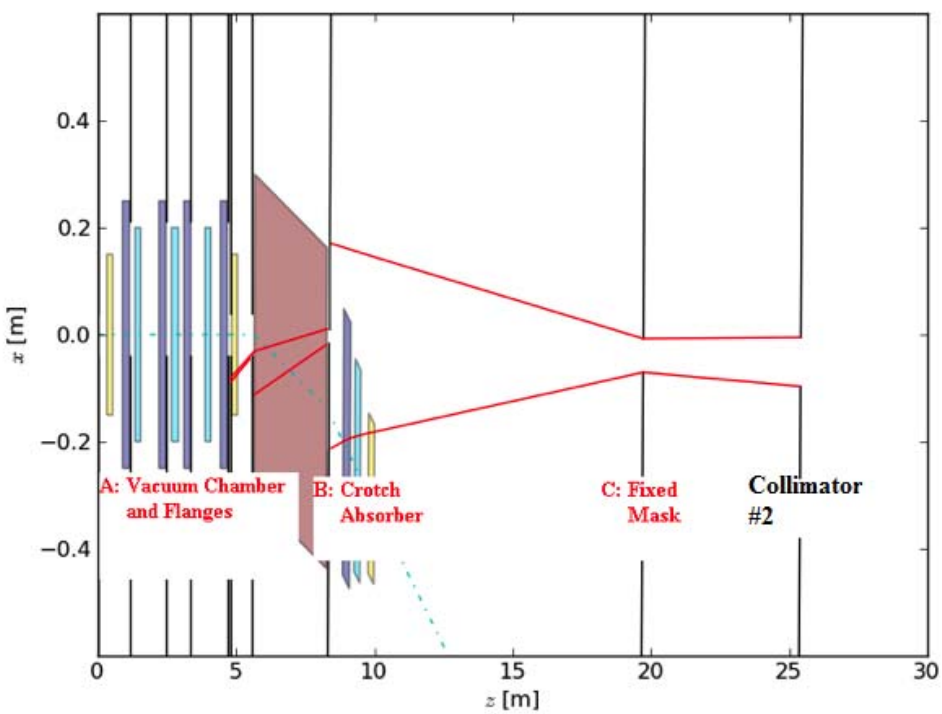

Figure 3.22 Backward tracking for a dipole beam-line

3.7.4.2 Robustness (safe margin) of interlocks

The robustness (safe margin) of interlocks on dipole field has been checked in the same way as before. After extending dipole field scan range to -35%, the beam-line is still safe (Figure 3.23). The reason why dipole/3PW beam-lines have larger safe margin than the XPD beam-line is that the crotch's outboard aperture is only 8mm, which constrains the worst trajectory position and angle.

The robustness of the injected beam energy interlock can be also checked as shown in Figure 3.24. The safety margin is much larger than the interlock limit +4%.

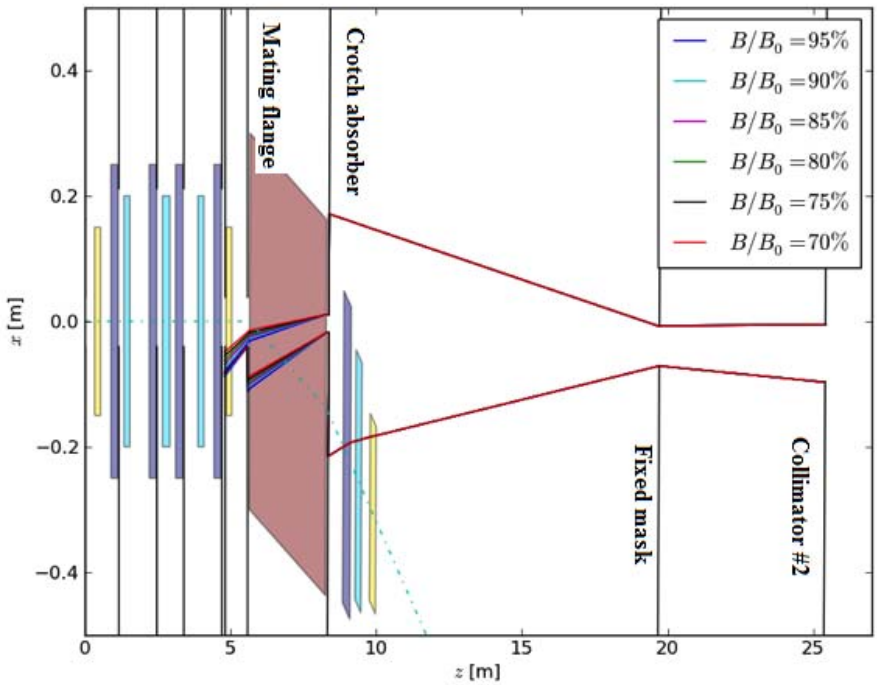

Figure 3.23 Robustness of dipole field interlock for dipole beam-lines

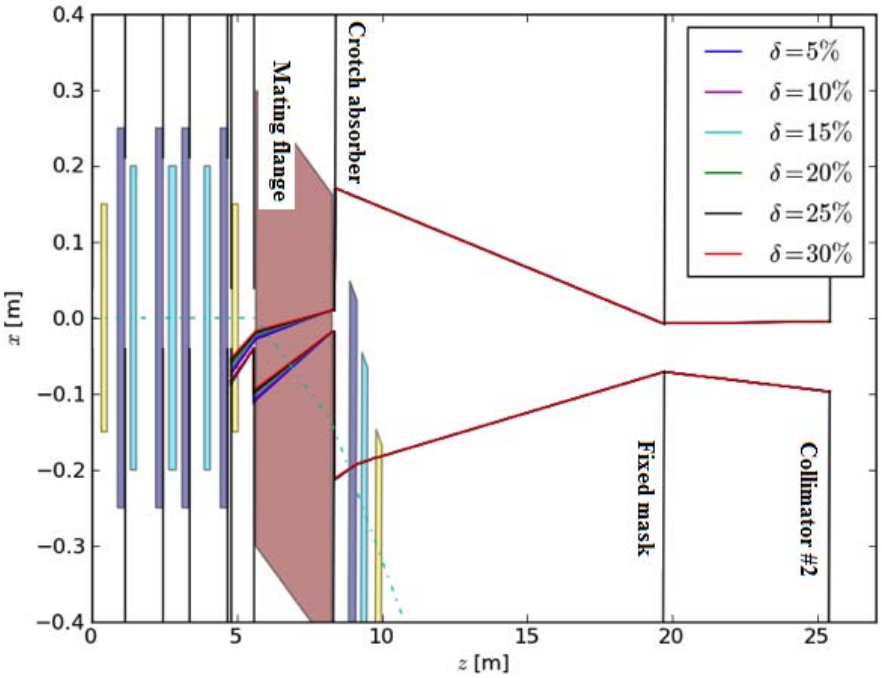

Figure 3.24 Robustness of injected beam energy interlock for the dipole beam-line

3.8 Summary of simulations

Backward tracking analysis using the cascaded parameter scan technique has been applied to study the safety of top-off injection for the six (seven) the NSLS-II project baseline ID beam-lines and the dipole/3PW beam-lines. All beam-lines are found to be safe with the required credited aperture configurations in place and the three interlock systems implemented. The interlocks on storage ring dipole power supply current and voltage, and booster ring dipole power supplies' currents have been shown to have wide safety margins for storage ring dipole field and injected beam energy.

As long as future beam-lines have apertures as restrictive as that for the XPD (at long straight) and the SRX (at short straight), they will be safe for top-off injection. As the designs of future beam-lines mature, they will be explicitly studied to assure they are safe for top-off injection.

Reference:

[1] M. Borland, L. Emery, Tracking Studies of Top-Up Safety at the Advanced Photon Source, Proceedings of the 1999 Particle Accelerator Conference, New York, 1999, Page 2319.

[2] H. Nishimura, et al., Advanced light source's approach to ensure conditions for safe top-off operation, NIM A, 608, 1, (2009).

[3] L. Emery, M. Borland, Analytical Studies of Top-Up Safety for the Advanced Photon Source Proceedings of the 1999 Particle Accelerator Conference, New York, 1999, Page 2939.

[4] NSLS-II front-end specification, http://groups.nsls2.bnl.gov/acceleratorsystems/mech/frontends/

[5] OPERA-2d&3d Reference Manual, Vector Fields Inc., http://www.vectorfields.com/opera.php

[6] X. Huang, et al, Tracking study for top-off safety validation at SSRL, NIM A, 635, 1, (2011).

[7] Y. Li, L. Yang and S. Krinsky, PRST-AB 14-3.

4.TOSS Magnet Interlocks System Requirements

The Top Off Safety Interlock System (TOSS) is design to keep various accelerator magnets within specified operating parameters to prevent the possibility of electrons going through the Storage Ring front end components into the beam lines outside the storage ring enclosure. Extensive calculations have been performed to determine the required magnet operating parameters. (The calculations are discussed in the previous section of this document.) If any of these operating parameters are outside allowable levels the TOSS will inhibit injection of the electron beam from the Booster Ring to the Storage Ring.

4.1 Magnet operating parameters requirements

Storage Ring - The maximum Storage Ring dipole magnet field variation is to be less than $\pm$ 5 % of 3.0 GeV operating level. There are three components that affect the field in each magnet. The first is the main current that flows through each magnet. The magnets are powered by a single power supply system. The second component is a dipole magnet trim coil. Each dipole magnet has its own individually powered trim coil. The maximum percentage adjustment of the field for the 35 mm dipole is $\pm$ 1% and the 90 mm dipole is $\pm$ 3%. The third component would be a magnet coil fault in the form of a turn to turn short. Since the 90 mm dipole trim coil is fixed at $\pm$ 3% then only $\pm$ 2 % is left for the current and shorted turn component of the interlock. The TOSS will incorporate sections for a $\pm$ 1% the Storage Ring dipole current interlock and a $\pm$ 1% for a Storage Ring dipole turn to turn short interlock. See Figure 4.1 for the Storage Ring Dipole Magnet Circuit.

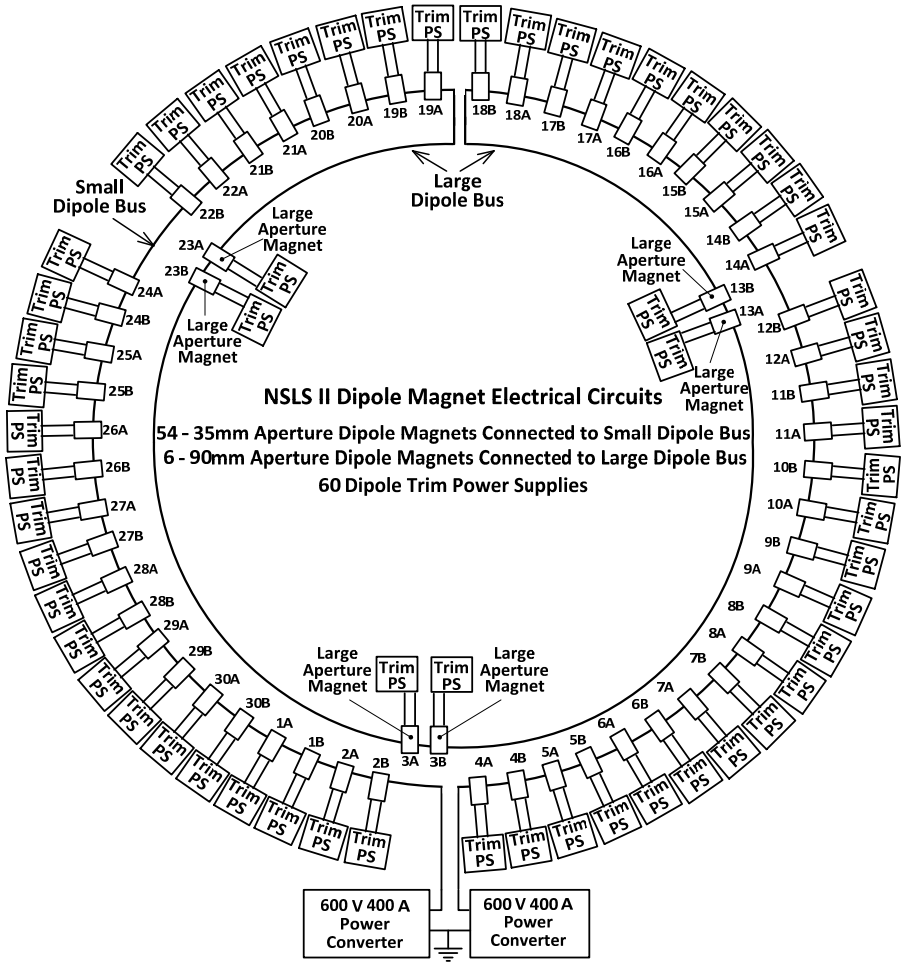

Figure 4.1 Storage Ring Main Dipole Circuit

Booster Ring - The Booster has three dipole magnet circuits. These three circuits have to ramp from low current (for injection into the booster) to a high current for extraction to the storage ring. The three power supplies' current must maintain a precise relationship between them for the electron beam to be accelerated to 3.0 GeV. The TOSS will incorporate a section for a ramping current interlock of $\pm$ 1%. There will be no turn to turn short interlock in the booster ring. This condition was ruled out because the beam will not be able to be accelerated in this fault condition. Also the likelihood that a turn to turn short will develop milliseconds before the beam is extracted is extremely small. See Figure 4.2 for the Booster Ring Dipole Magnet Circuits.

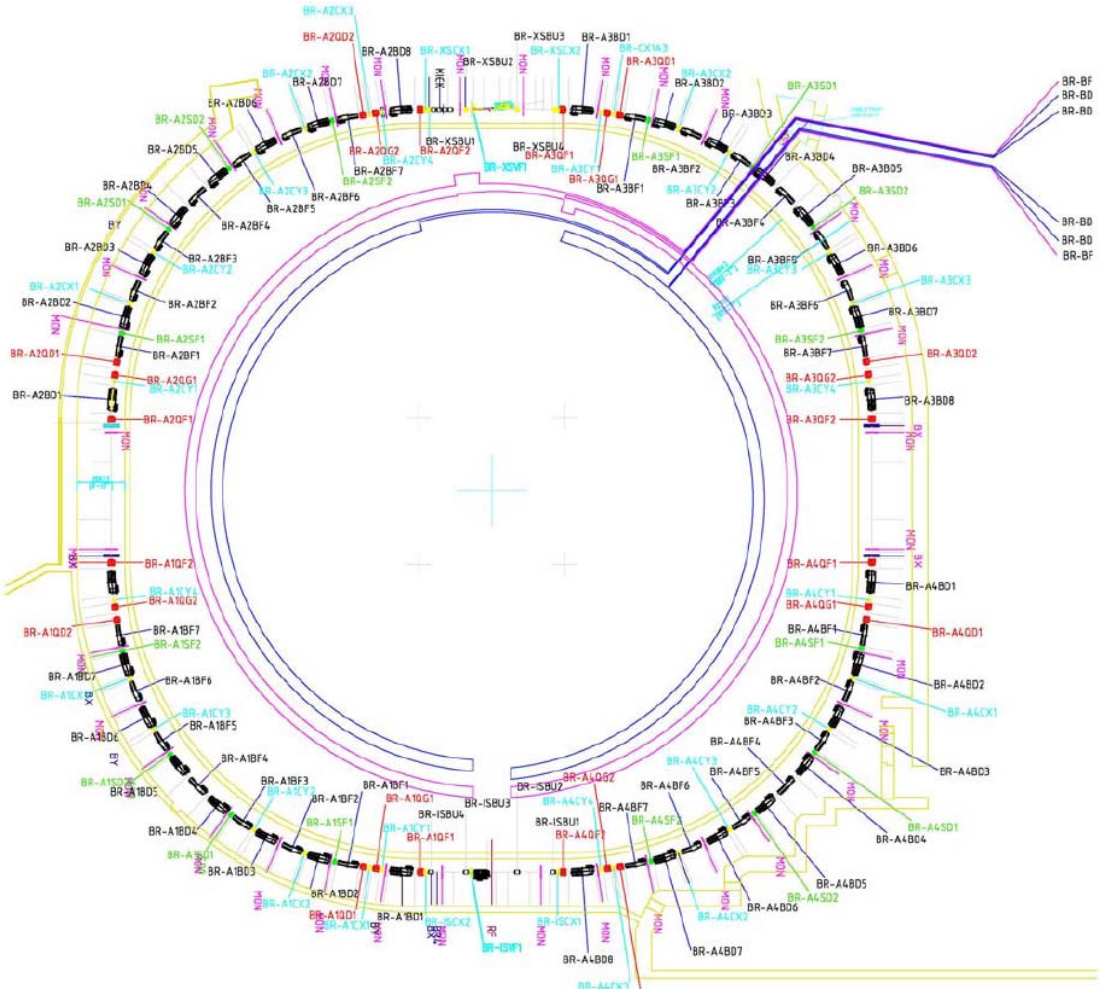

Figure 4.2 Booster Ring Dipole Magnets Circuits

4.2 Timing Requirements

The timing of the TOSS is a critical component for the system. The system must be able to determine the current of the Booster Ring dipole magnets be in a specified range only when it is at the extraction energy flat top. This will be for 15 milliseconds. The TOSS must resolve the measured current and determine if it is in the correct limits before allowing the beam is extracted from the booster. There also has to be some margin for adjustment when the beam can be extracted for proper operation of the accelerator. The two interlocks used in the storage ring will also have the same timing requirements. This will ensure that TOSS will be able to inhibit injection into the storage ring in milliseconds. Details of timing will be shown in Figure 4.3 for the storage ring dipole current and Figure 4.4 booster ring dipole current.

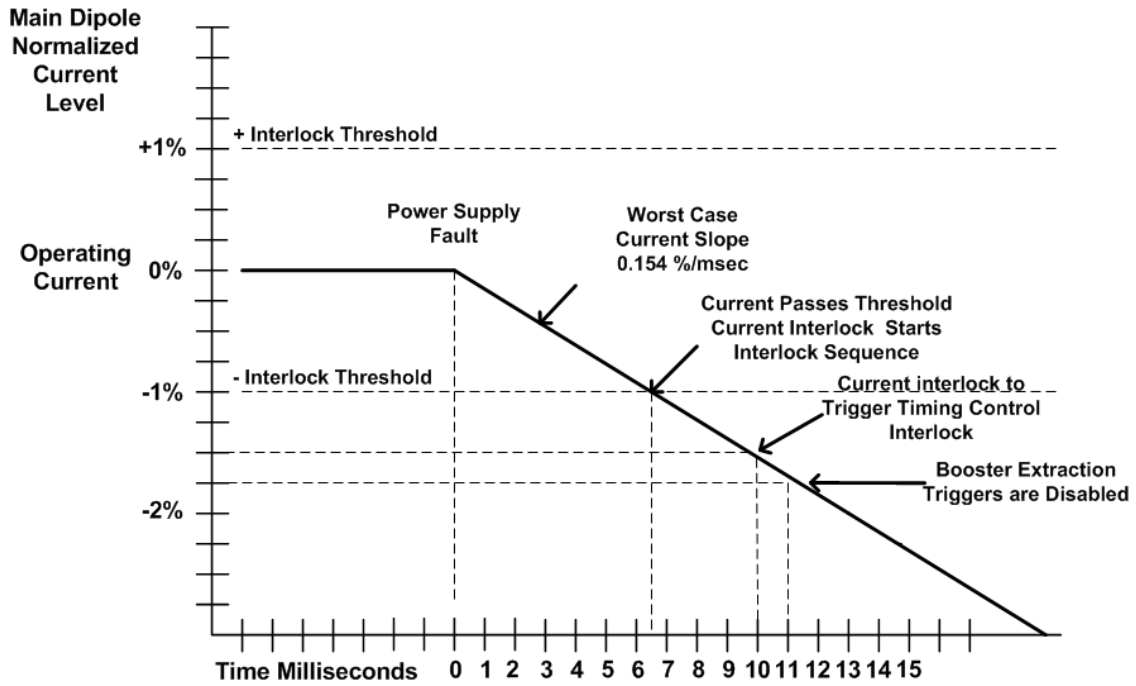

Figure 4.3 Storage Ring Dipole Current Interlock Timing Diagram

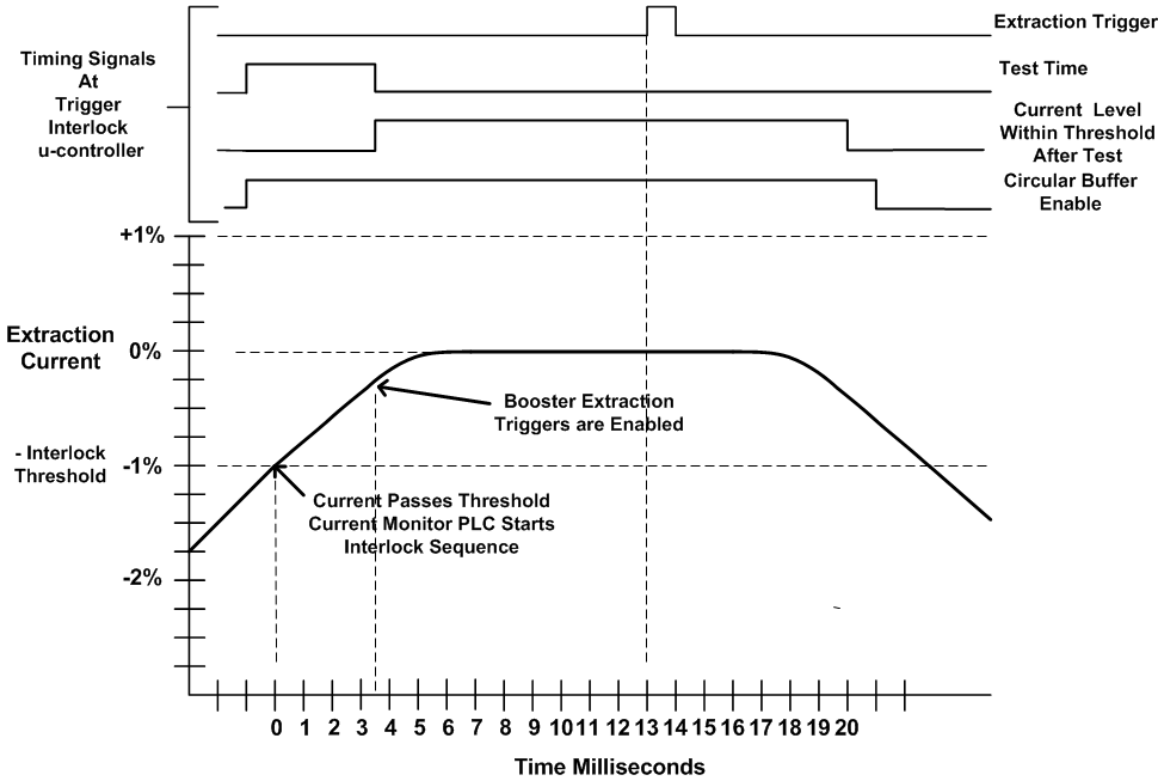

Figure 4.4 Booster Ring Dipole Current Interlock Timing Diagram

4.3 Interlock Requirements

The TOSS will inhibit the triggers from the control system to the Booster extraction AC septum and the storage ring injection AC septum. The TOSS will get

signals from the Storage Ring dipole current interlock, the Storage Ring dipole turn to turn short interlock, and the Booster dipole currents interlock. If all three interlock are satisfied the system will allow timing signals from the control system to pass through to trigger the extraction devices. These signals will be fast acting in the order of milliseconds. There will be two other inputs to the TOSS that will disable injection into the storage ring; they are the Accumulated Charge Monitor Interlocks (ACMI) for the Linac to Booster Transport Line (LBT) and the ACMI for the Booster to Storage Ring Transport Line (BST).

To enable the TOSS the two conditions must be satisfied. Operations personnel must enable the system for Top Off operations through the Storage Ring Front End PPS. The Storage Ring stored beam current must be above a specified minimum current. This will be determined by safety rated device that will interface to the Storage Ring Front End PPS. These signals through the Front End PPS are slow and are in the order of hundreds of milliseconds.

The TOSS will also allow Injection into the storage ring if the Front End PPS gives a signal that all Storage Ring front end shutters are closed. This will allow the Booster extraction triggers to pass through the TOSS. The operation of the Storage Ring shutters combined with the Front End PPS will make this control slow in the order of 2 to 3 seconds.

For operating the Booster with beam going to the booster dump, the TOSS must get a signal from the Booster PPS that the BS-B2 is at zero current and the BSTL safety shutter is closed. The control of the BS-B2 current is very slow. It will take tens of seconds to bring this power supply to zero. See Figure 4.9 for a logic diagrams for the TOSS interlocks.

Safety System Requirements:

- For TOSS sub-systems components should have a SIL 2 equivalence. This is requires by the radiation hazards if electron beam was to leave the Storage Ring enclosure. The systems will be designed with diverse and redundant components as required by the Photon Sciences Shielding Policy.
- An independent (external to BNL) analysis will be done to confirm the design.
- For sub-systems that require fast processing a safety rated micro-controller will be used. Two micro-controllers will be used in parallel and if practical from two different manufacturers or if from the same manufacturer they must be of a different design or construction.
- The two different micro-controllers will be configured in two separate chains with a different programmer for each chain. When interfacing to the safety PLC based PPS, the interface will be in both chains of the micro-controller and PLC. Only local programing will be implemented.
- Non-safety data will be transmitted through an isolated network to a data concentrator.
- The construction of the systems' hardware will meet all code and regulation for a safety system. This will include segregation and protection of signal cables,

tamper proof and lockable enclosures, and proper identification labels for all components.

- Documentation is to meet QA - A-1 level.
- The TOSS will have a test function built into the design to ensure proper operation. It will be incorporated into the normal operation of the sub-systems. The test will be milliseconds before the extraction of Booster beam.
- The TOSS will have provisions that will be designed into the different sub-systems to enable efficient certification of the system by ESH staff.

Diagnostic requirements:

Each of the sub-system micro-controllers will store data in two circular buffers in a ping pong configuration. Buffers will record all appropriate signals (Both analog and digital) during the time of booster extraction. The data will only be for 20 milliseconds with 333 microsecond sample period. Data in the buffers will be sent to the data concentrator at every extraction. A diagnostic application running in the data concentrator will alarm (the NSLS II control system) if an interlock condition has occurred. There will also be a controls screen that will enable viewing of all the stored data both in an immediate and archived mode. Archived data will be every data set that caused an interlock and at least one non-interlocked data set an hour. By having a data set every hour one would be able to look for possible trends that could cause the system to fault.

4.4 TOSS Interlock Design

The following are main design features for the TOSS Interlocks:

- Interlock speed is ~ 15 msec .
- The design will use safety rated micro-controllers.
- The micro-controllers will have a high scan rate with high resolution analog inputs that have a fast conversion speed. (~ 11 bits at 10 μs for voltage monitors and ~ 14 bits at 50 μs for current monitors)
- The design will use two different micro-controllers from TI. (See Figures 4.12, 4.13, 4.14, & 4.15 for a description on the micro-controllers) They will be configured very similar to the two chain design used in the Personal Protection System (PPS)
- The micro-controllers use the same developmental software systems. Each micro-controller chain will use a different programmer.
- Scan rate is estimated at ~ 100 μs scan rate and a total of 4 to 5 ms will be used determine an interlock condition (Main dipole) or safe for extraction condition (Booster dipole power supplies) (See timing diagrams)
- Programming of interlock thresholds will only be allowed by accessing local a programming port.
- Data will be stored in two circular buffer in the micro-controller for read out if an interlock condition occurs and when the top off occurs. This data will be transferred to a secured computer system that is used only for Top Off Safety System data collection. The secured computer is then interfaced to the NSLS II Controls Network.

- The NSLS II controls network will be isolated from the one used to collect data from the Top Off Safety System. (This is similar to the system that is used in the PPS.)
- The magnet interlock micro-controllers will signal (digital I/O) the Timing Control micro-controller through fiber optic cables. Each Magnet interlock Chassis will have it own interlock signal (A + B). The Timing Controller micro-controller will send a Test signal and a start Circular Buffer at Top Off (SCB).
- The critical devices that will inhibit injection into the storage ring will be safety rated interfaces that will block the trigger signals going into the booster extraction AC septum and storage ring injection AC septum.
- There will be isolated digital I/O for interlock signals coming from Accumulated Charge Monitors Interlocks (ACMIs) and Storage Ring Stored Current Interlock (SRSCI)
- Digital I/O s will be done through a safety designed fiber optics based system that will use a failsafe form of a frequency shift key circuit.
- Most of the components will be located in a tamper proof and locked chassis that will installed into one of the temperature controlled racks ($\pm$ 1 F) . This will maximize the stability of the micro-controller's ADC and the rest of the analog electronics.

For an overall block Diagram of the TOSS see Figure 4.5. This diagram will show all the connection to the different TOSS interlock chassis, PPS, critical devices, ACMI, and SRSCI.

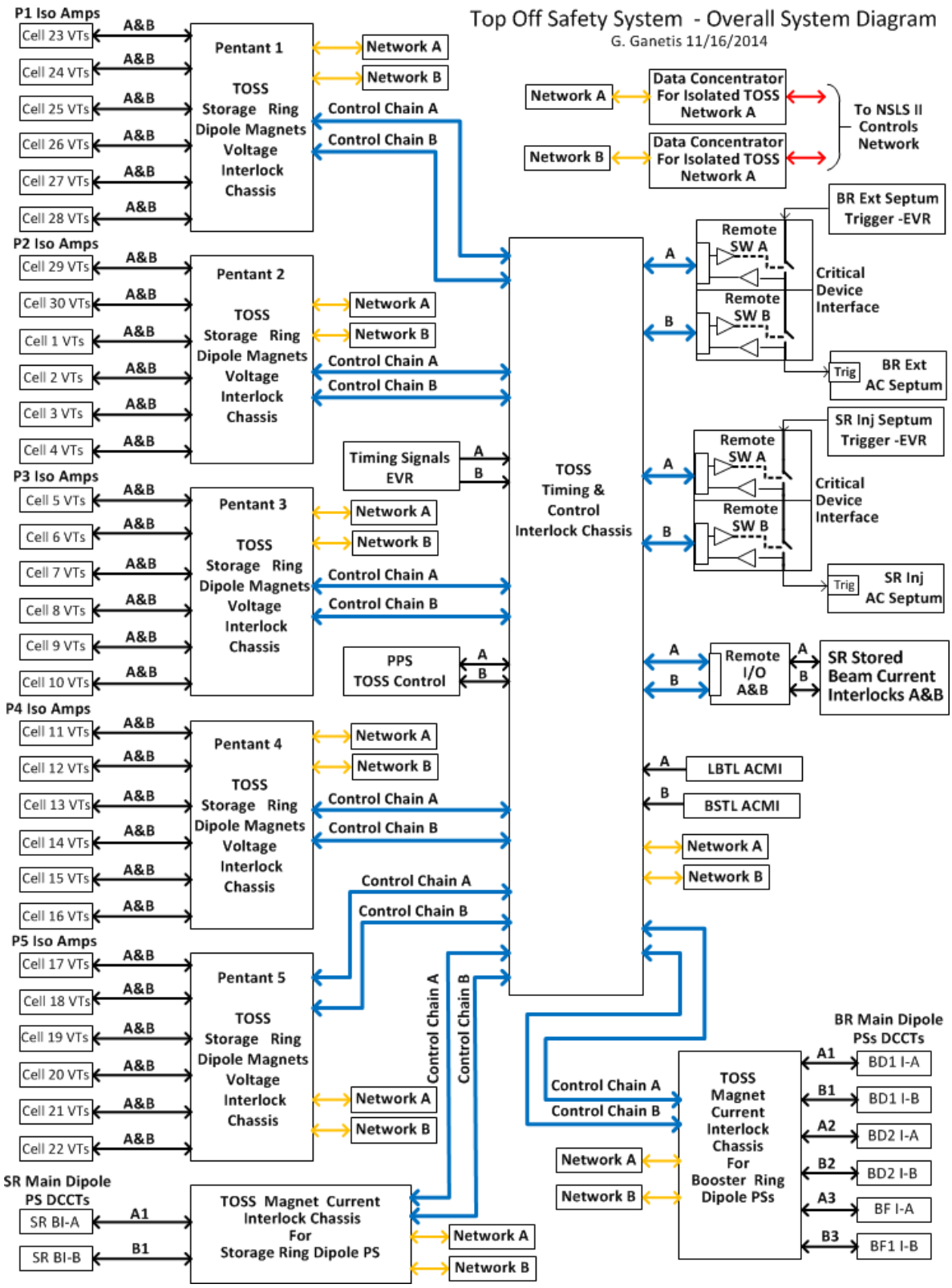

Figure 4.5 TOSS Overall System Diagram

4.5 Magnet Current Interlock

The following are the main design features that will be incorporated into the magnet current interlocks used on the storage ring and booster ring dipole magnet circuits:

- Two redundant DCCTs will be used on each power supply. The DCCTs will be from two different manufacturers, LEM Danfysik and Hitec.
- Different models is be used depending on the current range of the power supplies.
- All the DCCTs will use current output to minimize noise and improve accuracy. The output current of the DCCT head will be connected to a high precision burden resistors and scaling electronics. The components will produce stability of better then 5 ppm /C and have a time stability ~ 2 ppm/ month. The accuracy will be ~ 100 ppm and will be periodically checked using our metrology current standards (Certified by NIST at 10 ppm.)
- The DCCT heads will be mounted in a tamper proof locked cabinet located near the power supply cables. The burden resistor and scaling electronics will be located in the magnet interlock chassis. (See Figure 4.6 - Current Interlock Chassis block diagram.)
- Where possible different manufacturers and or models of burden resistor and scaling electronics will be used in the different chains (A & B).
- The bandwidth of the DCCTs and electronics will be ~ 10 kHz.
- Assuming ~ 14 bits ADC with $\pm$ 1 LSB , one gets 1 part in 8192 or 0.012% of full scale. The burden resistor and scaling electronics will be designed to utilize the full range of ADC.
- Cable routing will be done in segregated conduits or cable tray sections the same as the PPS.
- The DCCTs electronics have a system "OK" logic signal that will also be interlock by the mirco-controllers.
- For current signals that are fixed, a test feature will be used to make sure the signal is active by stimulating it with a known current change. This will happen before each top off.
- There will be key inputs to do a hardware reset for both chains of micro-controllers.
- There will be provisions for placing the micro-controllers in a certification mode.

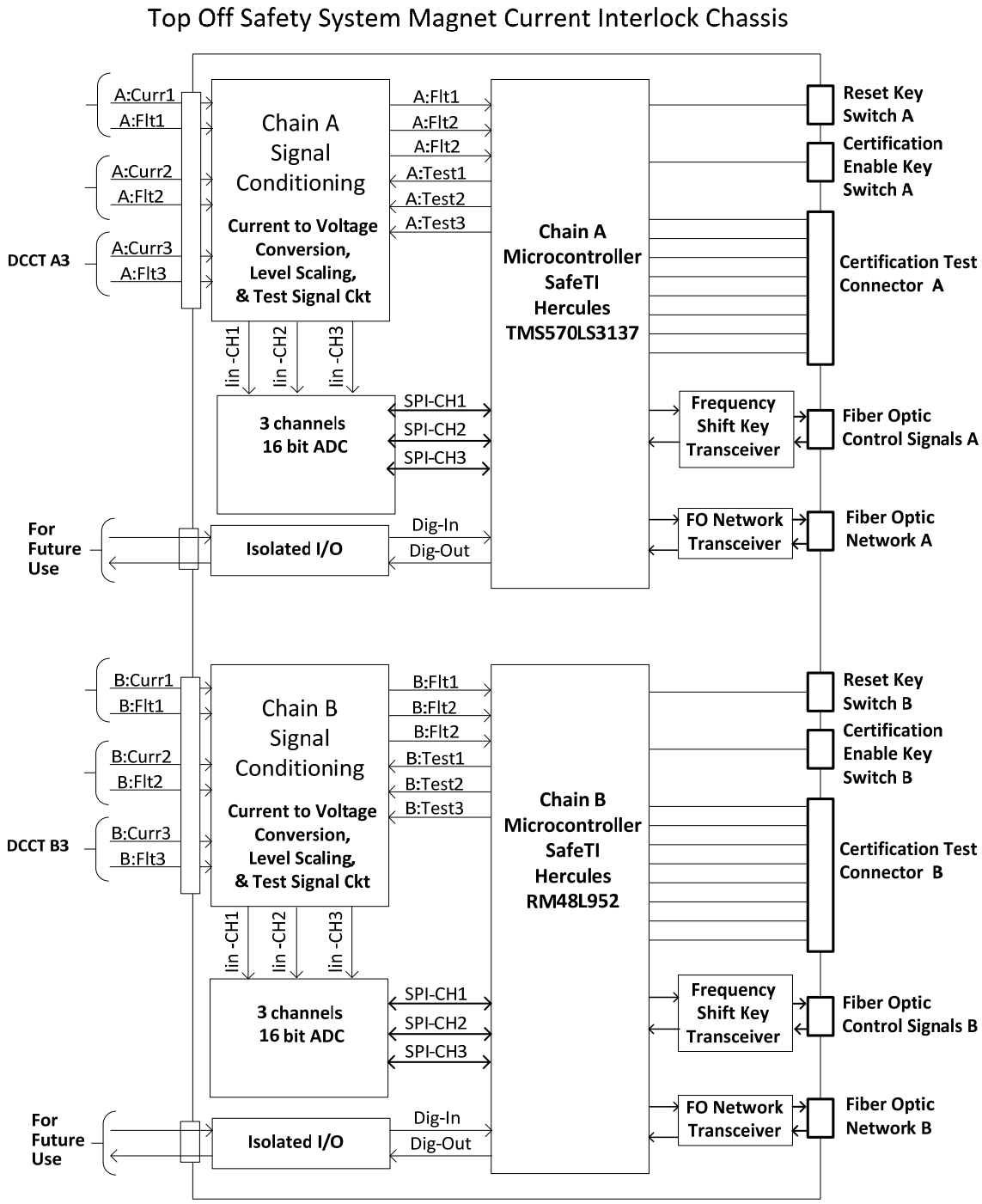

Figure 4.6 Current Interlock Chassis block diagram

4.6 Storage Ring Dipole Voltage Interlocks

The following are the main design features that will be incorporated into the magnet voltage interlocks used on the storage ring dipole magnet circuits:

- Voltage interlocks can be designed to detect a shorted turn or a 3% change in magnet voltage.
- A voltage difference method will be used to measure the voltage difference between each dipole in a Cell. This should take out the errors cause by temperature changes or differences in a cell or pentant. Each pentant has its own temperature control and there could be slight temperature differences (1.0 C) between pentants.
- A multi-channel (chains A & B) voltage measurement electronics will be designed for the main dipole circuit. This design will measure the voltage across dipole magnet. The signal will be isolated and buffered and scaled to safe levels in the Isolation Amplifier Chassis which is located in each cell. (See Figure 4.7 – Isolation Amplifier Chassis Diagram)
- The multi-channel voltage interlock chassis electronics will be located at the center of each pentant and have a total of 12 inputs. It will be in a temperature controlled rack so it will have high stability. The chassis that it will be located in will be tamper proof and locked. (See Figure 4.8 – Dipole Magnet Voltage Interlock Chassis)
- There are two dipole magnets in each cell, each 35 mm dipole has 32 turns so a single shorted turn is 1 part in 64 or 1.52 %. The system electronics will be scaled so the micro-controller's ADC with a resolution of 0.012% should be able to determine a hard single turn short using the difference signal. The raw signals will also be inputted into the system for consistency checks and for diagnostics.
- The voltage signal is fixed so a test feature will be used to make sure the signal is active by stimulating it with a known voltage change at the isolation amplifiers. This will happen before each top off.
- The 90 mm dipole will use a similar system that will take the difference between two 90 mm dipoles that are located in a cell. Each 90 mm dipole has 84 turns. There are two dipole magnets in a cell, each 90 mm dipole has 84 turns so a single shorted turn is 1 part in 168 or 0.59 %. The system electronics will be scaled so the PLC's ADC with a resolution of 0.012% will be able to determine a hard single turn short using the difference signal. There are three locations around the storage ring where the 90 mm dipoles magnets are located. (Cells 3, 13, & 23)
- There will be key inputs to do a hardware reset for both chains of micro-controllers.
- There will be provisions for placing the micro-controllers in a certification mode.

4.7 Isolation Amplifiers for Storage Ring Dipole Magnets

The isolation amplifiers have a test feature where the signal is changed right before the top off system is needed to confirm the voltages are operational. The output of the amplifiers is a current signal to minimize noise getting into the signal. Current limiting resistors will be installed at the magnet to prevent damage of the cabling if there is a short to ground. Each chassis will have both chains A & B in it. Chain A will use an isolation amplifier from the same manufacturer and chain B will use one from a different manufacturer

.

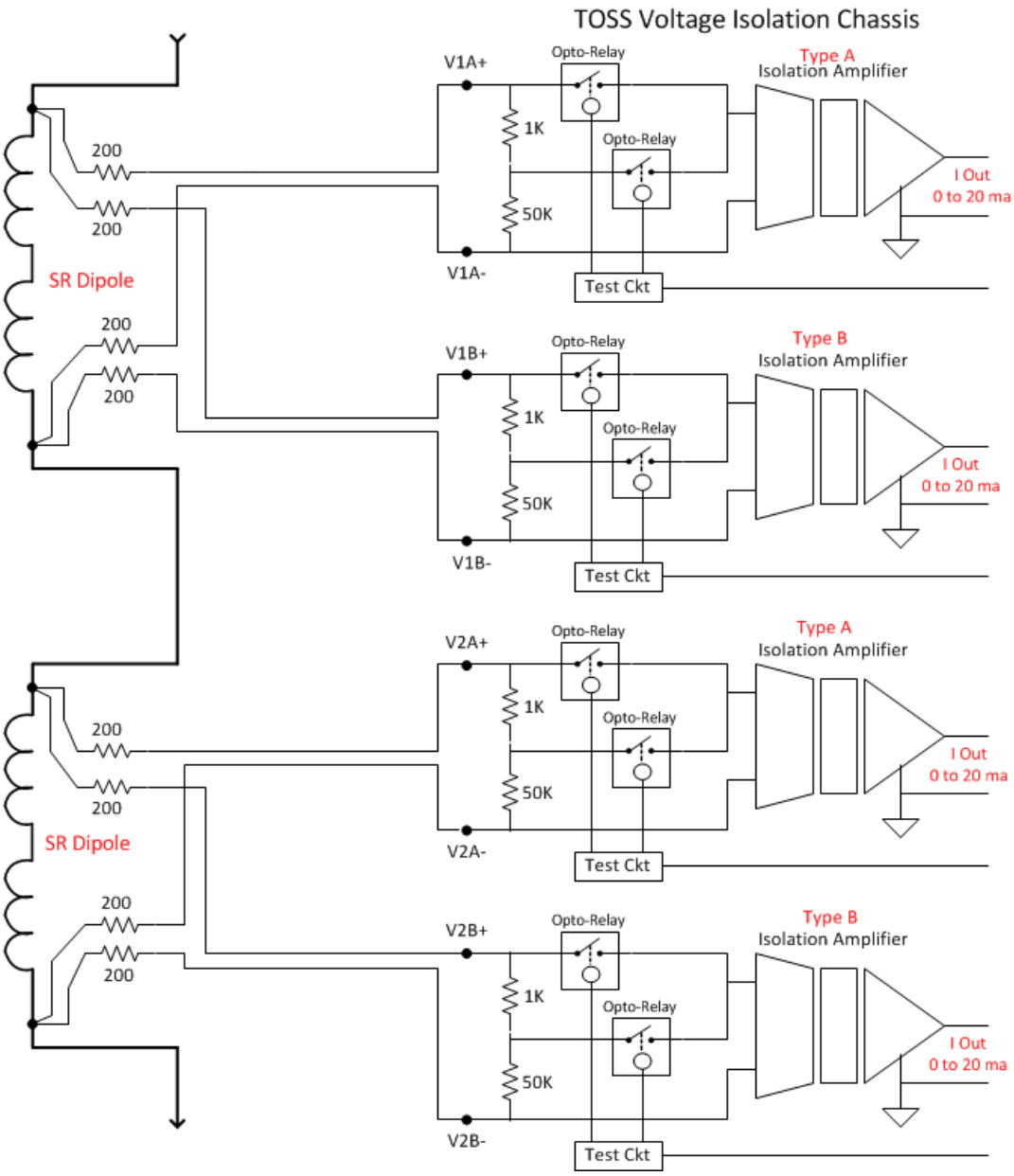

Figure 4.7 Isolation Amplifier Chassis Diagram

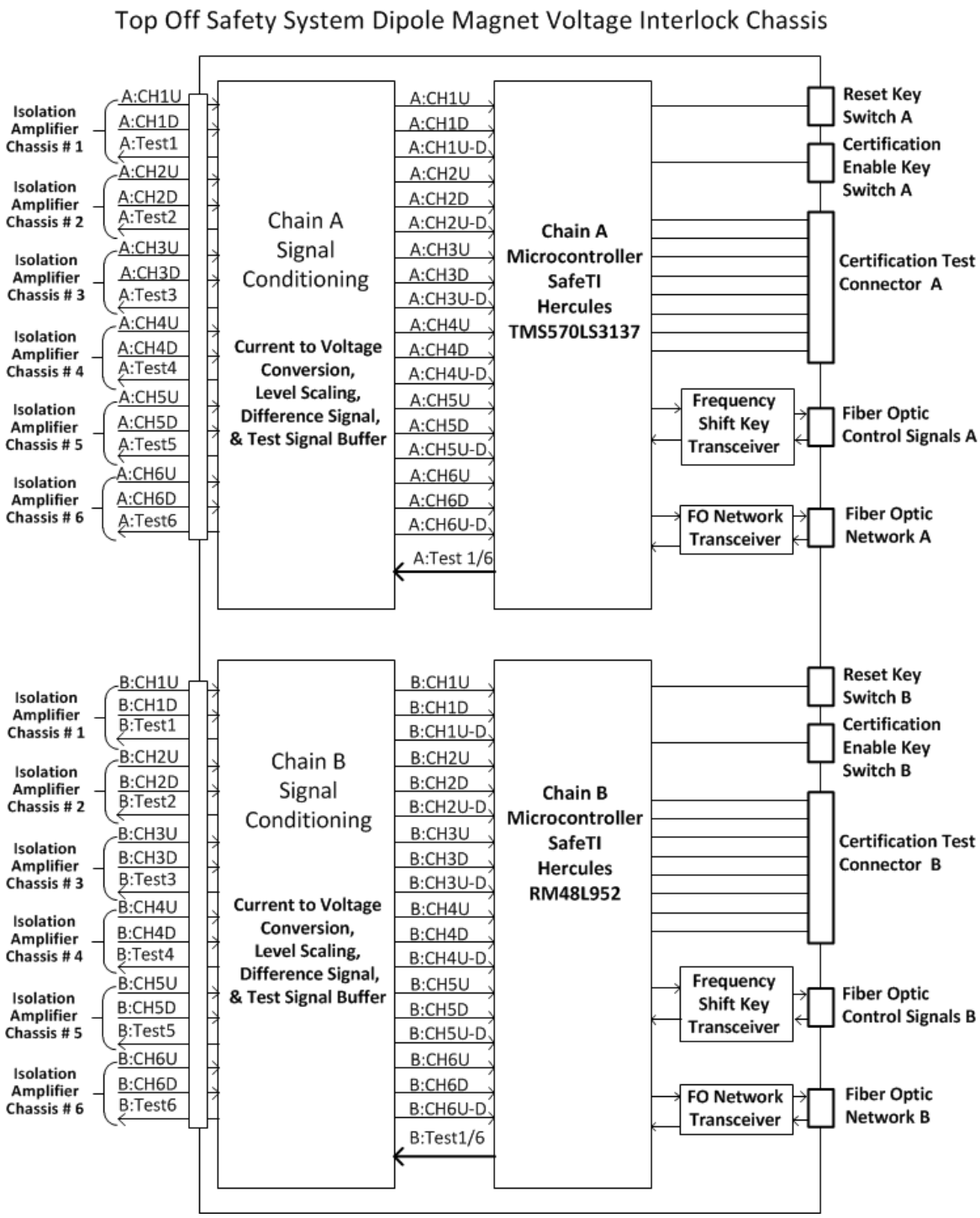

Figure 4.8 Dipole Magnet Voltage Interlock Chassis

The following figures are preliminary logic diagrams that will be implemented in the Timing Control Chassis. The Timing Control Chassis performs the main interlock functions of the TOSS:

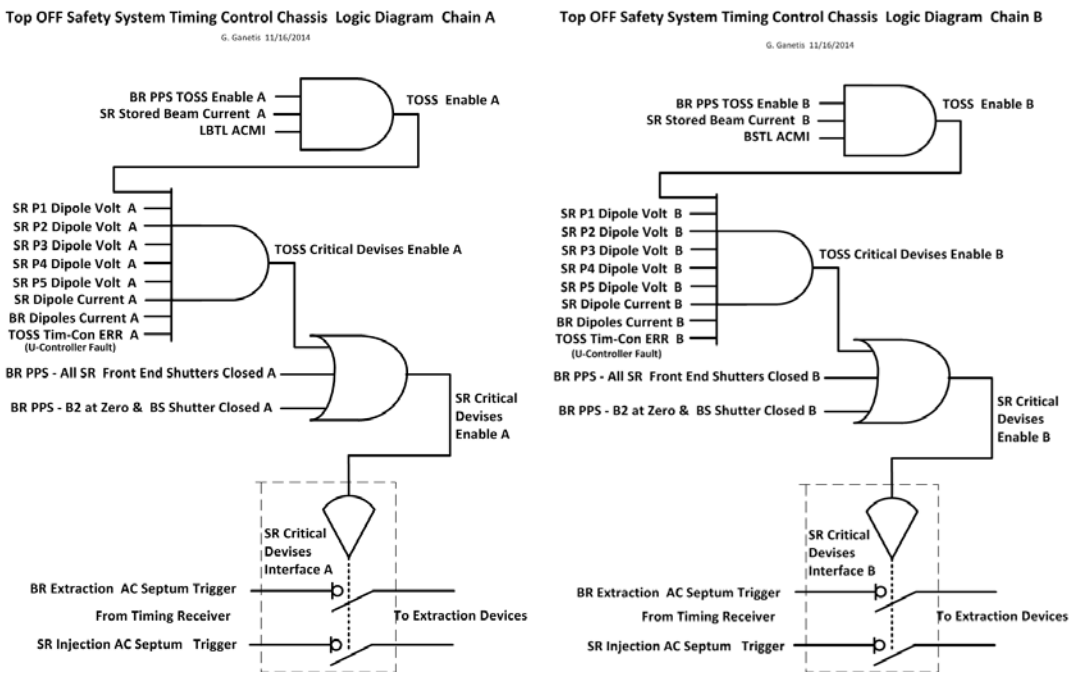

Figure 4.9 Logic Diagrams for Timing Control Chassis - Chains A & B

The following figures are preliminary logic diagrams that will be implemented in the TOSS Current Chassis for both the booster and storage ring: (The current chassis preforms the interlock function if the currents of the magnet circuits are not within their limits.)

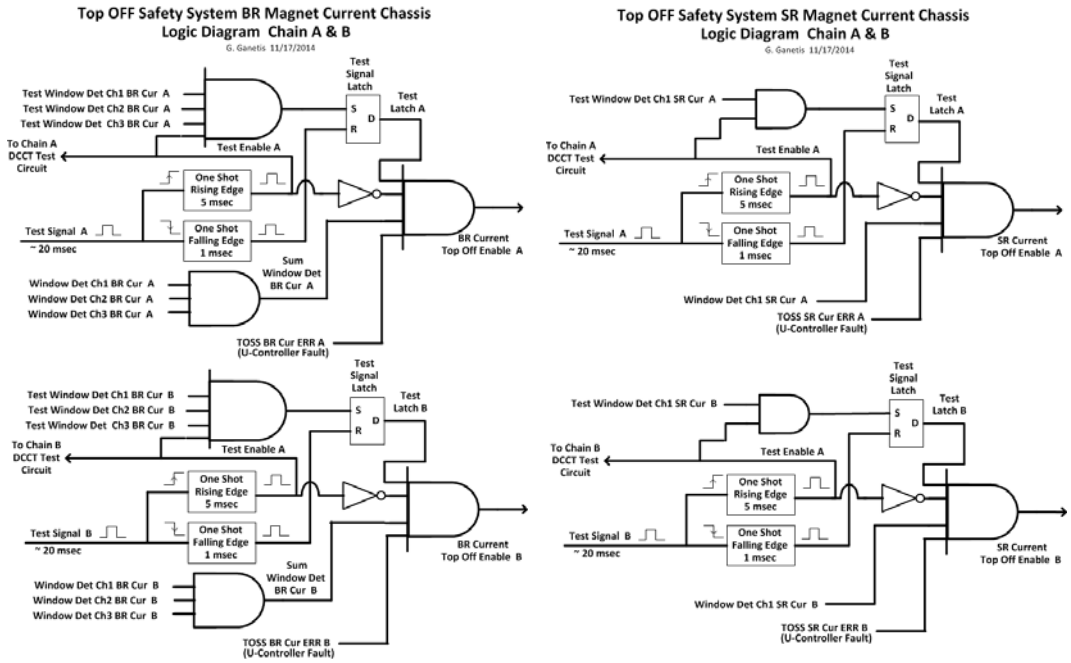

Figure 4.10 Logic Diagrams got TOSS Current Chassis for Storage and Booster Dipole Magnets

The following figures are preliminary logic diagrams that will be implemented in the TOSS Voltage Chassis for the storage ring: (The voltage chassis preforms the interlock function if the dipole magnet voltages are not within their limits.)

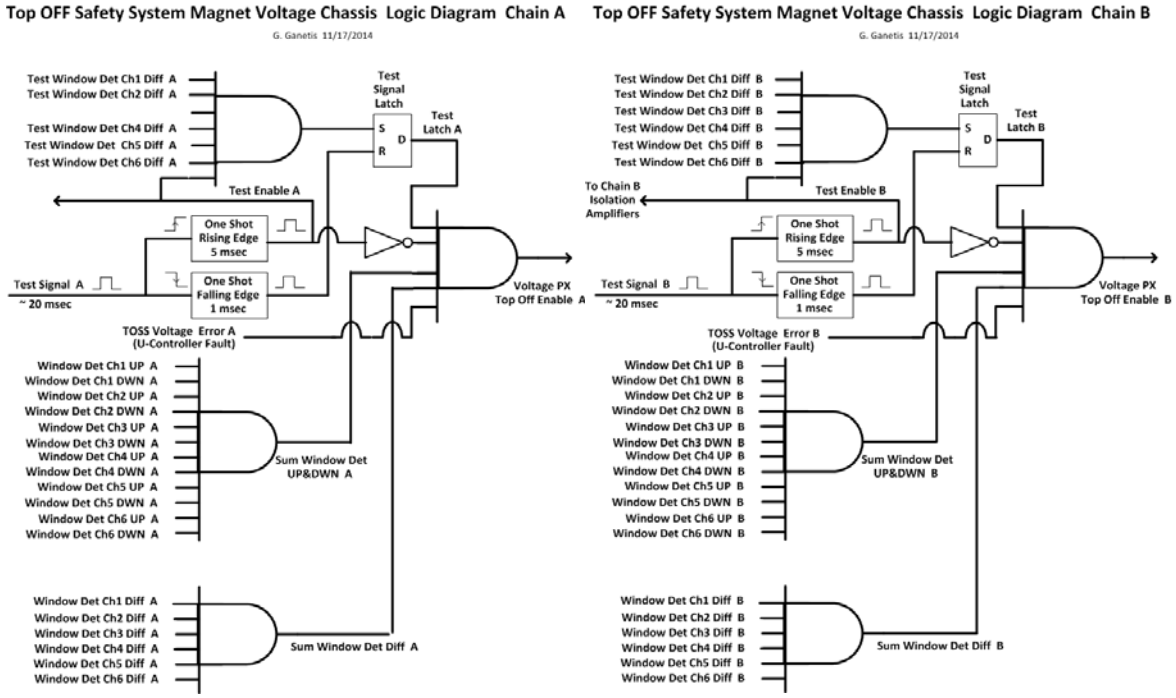

Figure 4.11 Logic Diagrams got TOSS Voltage Chassis for Storage Dipole Magnets

4.8 MicroController

The interlocks for TOSS is using two different versions of the Texas Instruments (TI) Family of safety rated micro-controllers. These devices are used in life safety application in transportation and medical. This design is planning to use evaluation boards from TI since our hardware requirements are relativity simple. The boards are similar bur use different micro-controllers. The boards will allow easy interface to the external circuits that will be required to interface to the rest of the TOSS components.

A side by side comparison shows the features are very similar between the two micro-controllers. The difference is the chip is a completely different die. This should give the diversity one should have in a safety rated system.

Hercules Safety Rated Micro-Controllers

J#	Function
J1	Ethernet
J2	DCAN1
J3	DCAN2
J4	JTAG header
J6	Mictor RTP
J7	Mini-B USB
J9	SPI1, ADC
J10	EXP P2, SPI2
J11	SPI3, GIO
J12	Mictor DMM
J15	SD card
J16	Type B USB
J17	Type A USB
J18	Type A Host
J19	MIPI Header
P1	+12 V In

TI Micro- Controller MS570LS3137

- **Transportation Applications**
- **-40 to 125 ºC Operation**
- **IEC61508 SIL-3 & ISO26262 ASIL-D**
- **Dual CPUs in Lockstep**
- **CPU Logic Built in Self Test (LBIST)**
- **Flash & RAM w/ ECC**
- **Memory Built-in Self Test (PBIST)**
- **Cyclic Redundancy Checker module**
- **Ethernet connectivity**
- **2 x12-bit Multi-Buffered ADC**
- **24 total input channels (16 shared)**
- **Calibration and Self Test**
- **5 SPI (3 Multi-Buffered)**
- **Cortex-R4F over 280 DMIPS**
- **Supported by SCIOPTA - Real-Time Operating System certified to IEC61508/EN50128 by TÜV.**

TI Micro Controller RM48L952

- **Industrial/Medical Applications**
- **-40 to 105 ºC operation**
- **IEC61508 SIL-3**
- **Dual CPUs in Lockstep**
- **CPU Logic Built in Self Test (LBIST)**
- **Flash & RAM w/ ECC**
- **Memory Built-in Self Test (PBIST)**
- **Cyclic Redundancy Checker module**
- **Ethernet connectivity**
- **2 x12-bit Multi-Buffered ADC**
- **24 total input channels (16 shared)**
- **Calibration and Self Test**
- **5 SPI (3 Multi-Buffered)**
- **Cortex-R4F over 350 DMIPS**
- **Supported by SCIOPTA - Real-Time Operating System certified to IEC61508/EN50128 by TÜV.**

Device series	TMS570LS3137	RM48L952
CPU Core	Lockstep Dual Cortex-R4F	Lockstep Dual Cortex-R4F
Flash Memory Size	2MB – 3MB	2MB – 3MB
SDRAM	8MB	8MB
Floating Point	IEEE	IEEE
ADC	2x 12 bit	2x 12 bit
Ethernet	10/100 Mbps	10/100 Mbps
USB	No	FS Host, Device
ECC on Flash & RAM	Yes, evaluated in CPU	Yes, evaluated in CPU

Figure 4.12 Comparison of features the two safety rated micro-controllers used in TOSS

TOSS will use a well-developed operating system that is used in safety rated micro-controllers. The interlock logic is straight forward and the data acquisitions requirements are well within the capabilities of the software. It also allows higher level functions and data storage that will be used in diagnostic features of the system.

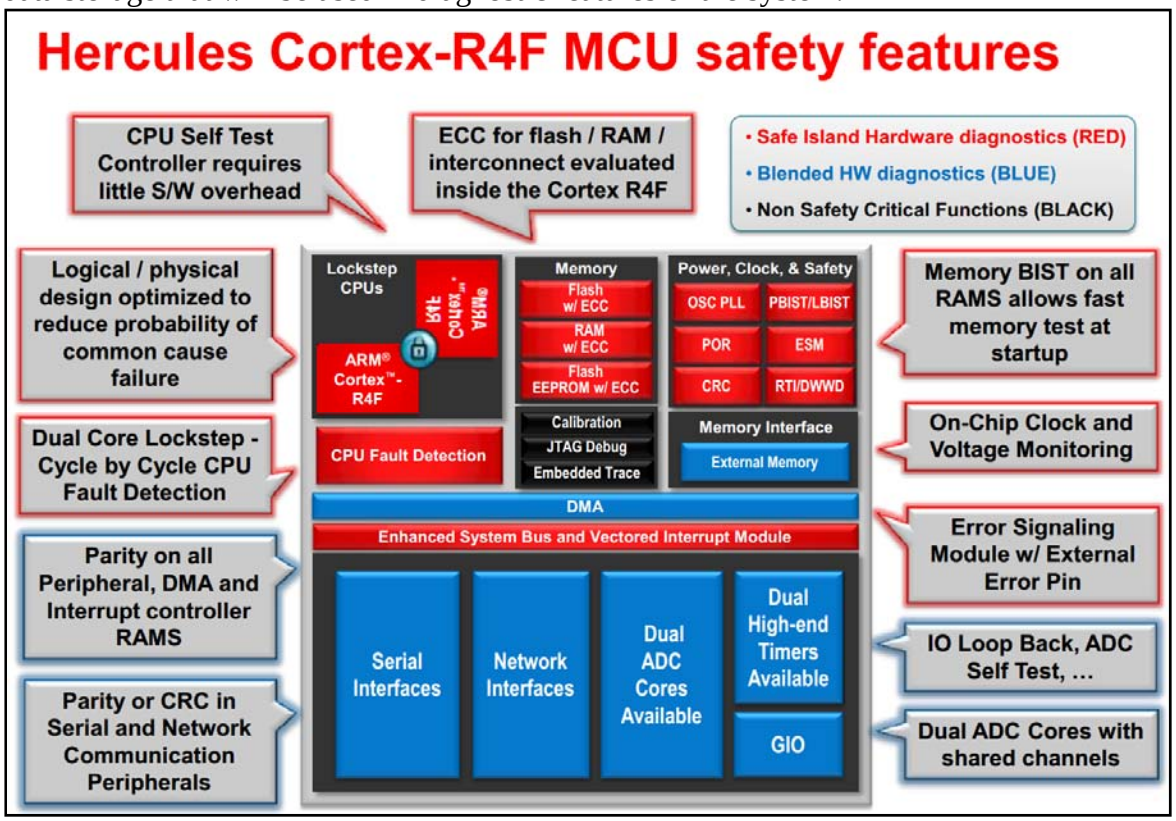

Figure 4.13 Safety software features for the micro-controllers used in TOSS

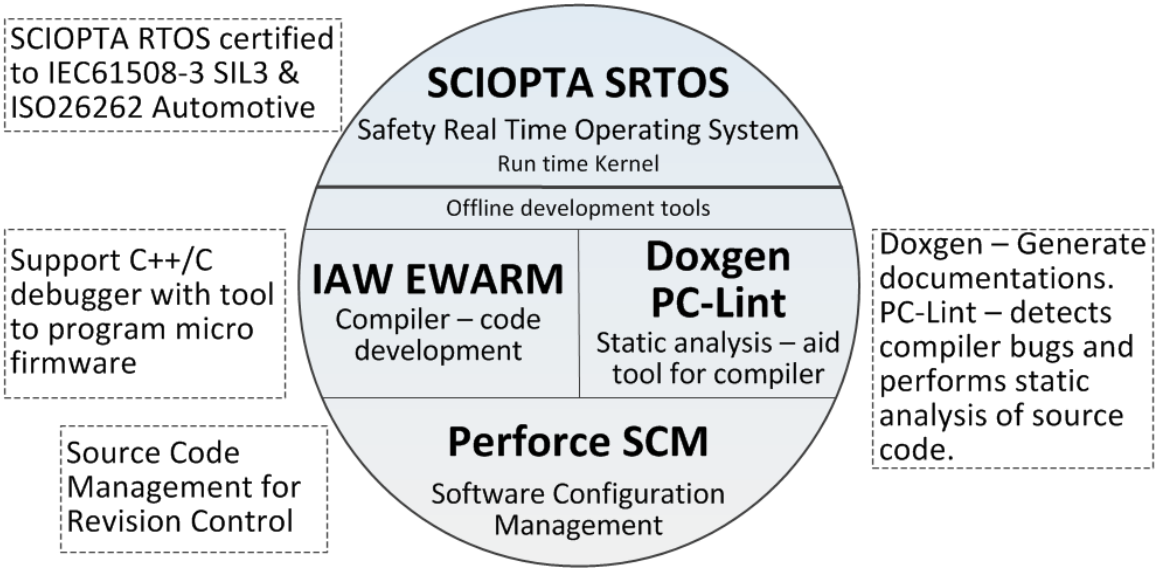

Figure 4.14 Safety software features for the micro-controllers used in TOSS